MOLECULAR AND CELLULAR BIOLOGY
2023, VOL. 43, NO. 9, 451–471
https://doi.org/10.1080/10985549.2023.2239694

Taylor & Francis
Taylor & Francis Group

RESEARCH ARTICLE

Degradation of CDK9 by Ubiquitin E3 Ligase STUB1 Regulates P-TEFb Level and Its Functions for Global Target Gene Expression within Mammalian Cells

Subham Basu,[a]* Arijit Nandy,[a,b]* Avik Ghosh,[a]* Dheerendra Pratap Mall,[a] Debabrata Biswas[a,b]

[a]Laboratory of Transcription Biology, Molecular Genetics Division, CSIR-Indian Institute of Chemical Biology, Kolkata, India
[b]Academy of Scientific and Innovative Research (AcSIR), Ghaziabad, India

ABSTRACT Positive transcription elongation factor b (P-TEFb) regulates expression of diverse sets of genes within mammalian cells that have implications in several human disease pathogeneses. However, mechanisms of functional regulation of P-TEFb complex through regulation of its stability are poorly known. In this study, we show an important role of C-terminus of Hsc70-interacting protein (CHIP aka STUB1) in regulation of overall level of CDK9 and thus P-TEFb complex within mammalian cells. STUB1 acts as a ubiquitin E3 ligase for proteasomal degradation of CDK9 involving N-terminal lysine 3 (K3) residue. Whereas, overexpression of STUB1 enhances, its knockdown reduces overall CDK9 degradation kinetics within mammalian cells. Interestingly, owing to the same region of binding within CDK9, CyclinT1 protects CDK9 from STUB1-mediated degradation. Factors that cooperatively bind with CyclinT1 to form functional complex also protects CDK9 from degradation by STUB1. Knockdown of STUB1 enhances CDK9 expression and thus P-TEFb complex formation that leads to global increase in RNA polymerase II CTD phosphorylation and transcriptional activation of diverse P-TEFb target genes. Thus, we describe an important functional role of STUB1 in regulation of transcription through modulation of overall level of P-TEFb complex formation within mammalian cells.

KEYWORDS CHIP, STUB1, ubiquitination, CDK9, P-TEFb complex, transcription, RNA polymerase II

INTRODUCTION

Depending on context, mammalian cells respond to external cues by activating or repressing sets of genes for optimal response and overall survival. Among all the positive regulators of transcription, P-TEFb complex plays an important role in overall functional regulation.[1–3] Human P-TEFb complex is a heterodimer composed of CyclinT1/2 and cyclin-dependent kinase, CDK9.[4,5] The majority of the cellular P-TEFb complex within mammalian cells remain in an inactive form in association with HEXIM1, LARP7, MePCE2 and 7SK snRNA to form the 7SK snRNP complex.[6,7] Upon external stimulation, the P-TEFb complex is dissociated from the 7SK snRNP complex to associate with various other positive regulators of transcription including p53, BRD4, ZMYND8 as well as components of super elongation complex (SEC) to be recruited at promoter proximal region for transcriptional activation.[3,8–11] Upon its recruitment at the promoter proximal region, P-TEFb complex phosphorylates components of Negative Elongation Factor (NELF), DRB-Sensitivity Inducing Factor (DSIF) as well as conserved Ser2 and Ser5 residues of C-terminal heptad repeats of RNA polymerase II (Pol II, hereafter) for releasing paused Pol II for transcriptional activation.[12]

Supplemental data for this article can be accessed online at https://doi.org/10.1080/10985549.2023.2239694.

Address correspondence to Debabrata Biswas, dbiswas@iicb.res.in.

*These authors contributed equally to this work.

The authors declare no conflict of interest.

Received 15 April 2023
Revised 6 July 2023
Accepted 18 July 2023

Although mechanisms of P-TEFb-mediated transcriptional activation in association with other factors have been well elucidated, unexpectedly, functional regulation of P-TEFb complex through regulation of stability of its components have been poorly known. The role of E3 ubiquitin ligase SKP2 in regulation of CDK9 level for optimal Tat-dependent transcriptional activation has been described a while ago.[13,14] Both these studies showed that CyclinT1-dependent recruitment of SKP2-containing SCF complex regulates the level of CDK9 protein through its ubiquitination. However, same CyclinT1 component being involved in functional P-TEFb complex formation as well as degradation of CDK9, lead to the overall mechanistic understanding less clear. However, no other studies, to our knowledge, have elucidated a role for other ubiquitin E3 ligase(s) in regulation of CDK9 protein level and thus functions of P-TEFb complex. In this study, we have described a critical role of STUB1 (STIP1-homology and U-Box containing protein 1) in regulation of CDK9 level and thus overall P-TEFb complex formation for regulation of target gene expression within mammalian cells.

The human CHIP/STUB1 is an U-box containing ubiquitin E3 ligase whose functional activity has predominantly been described in the context of Hsp70 and Hsc70 cochaperone complexes.[15] Multiple studies demonstrated the role of STUB1 as a protein mediating target polyubiquitylation in a chaperone-dependent manner, including c-ErbB2, Smad1, the tau protein, SOD1, E2A proteins (E12 and E47), neuronal NOS, ASK1, α-synuclein and even the R175H gain of function mutant of p53.[16–23] As STUB1 was identified initially as an Hsc70 interacting protein, multiple groups reported the significant role it could play in the heat shock response. Upon heat stress, STUB1 was found to interact directly with HSF1 and prevent apoptosis.[24,25] Upon attenuation of HSF1 activity, STUB1 regulates the degradation of the heat shock response proteins to maintain them at physiological concentrations.[26] STUB1 protein contains multiple TPR domains that are predominantly involved in protein-protein interaction. The ubiquitin E3 ligase function is attributed to the U-box domain present within the protein.[27]

Along with its role in maintenance of protein quality control, STUB1 has also been shown to play an important role in the development of malignancies. The first clue for this regulation emerged when STUB1 was observed to degrade ErbB2, the overexpression of which contributes to multiple human cancers.[28] An elegant study also showed the role of STUB1 in preventing cancers by the ubiquitylation of oncogenic proteins. Indeed, knockdown of STUB1 resulted in the enhanced expression of SRC-3, ACTR15, TRAM-1, p/CIP17 and RAC3, giving rise to increased proliferation, anchorage independent growth and invasiveness in breast cancer cell lines.[29] Analysis of the role of STUB1 in different cancers seems to indicate a dual property, wherein STUB1 acts as a tumor suppressor in certain cancers, while in others, it is able to enhance malignant growth. For example, analysis of STUB1 expression in gastric cancer patients indicated its lower levels correspond to shorter life expectancies. Here, STUB1 was observed to be interacting with NF-κB/p65, and causing its degradation, thereby inhibiting IL-8 induced angiogenesis.[30] Low levels of STUB1 also corresponds to enhanced YAP1 levels, which promotes the Hippo signaling pathway, thereby promoting cancer cell survival and chemoresistance.[31] The histone demethylase JMJD1A has been shown to regulate activities of the androgen receptor and promote prostate cancer. Castration resistant prostate cancers show high JMJD1A activity with low STUB1 levels. JMJD1A stability is obtained by p300 mediated acetylation which prevents its degradation by STUB1.[32] Hence, STUB1 in prostate cancer resulted in the degradation of the androgen receptor and leading to arrest of cells in the G1-S phase of mitosis.[33]

In an effort toward identifying other E3 ubiquitin ligase(s) that could play potential role in regulation of CDK9 level, we were intrigued by the observation of CDK9 association with STUB1. Detailed mechanistic analyses showed that STUB1 regulates CDK9 level within mammalian cells through polyubiquitination at the conserved lysine 3 (K3) residue at its N-terminus. Functional implication of this mechanism of CDK9 regulation in transcriptional activation for target gene expression is detailed in this study.

RESULTS

STUB1 is a novel CDK9-interacting protein. In order to identify potential novel regulator of CDK9 that could be involved in its functional regulation within mammalian cells, we generated a stable cell line that ectopically expresses human CDK9 as FLAG-HA-tagged.[3,34] Purification of CDK9-associated proteins using the nuclear extract of this stable cell line and subsequent mass spectrometry analysis identified STUB1 as a novel interactor of CDK9 (Fig. S1A). Subsequent immunoblot analyses further confirmed CDK9 interaction with STUB1 along with other known interactors within mammalian 293T cells (Fig. 1A, lane 3). To address this interaction in endogenous context, our subsequent immunoprecipitation analysis using specific antibody also confirmed CDK9 interaction with endogenous STUB1 (Fig. 1B, lane 3). A reciprocal immunoprecipitation analysis using ectopically expressed STUB1 further confirmed CDK9 interaction along with its known interaction with Hsp70 (Fig. 1C, lane 3). Interestingly, in these interaction analyses, we failed to observe STUB1 interaction with other component of P-TEFb complex i.e. CyclinT1. Further, we also failed to observe STUB1 interaction with SEC components such as ELL. Similar results have also been observed in endogenous context wherein immunoprecipitation of endogenous STUB1 with specific antibody showed interaction with CDK9 and Hsp70, however, failed to show interaction with CyclinT1 as well as SEC component ELL (Fig. 1D, lane 2).

Next, we addressed whether CDK9 directly interacts with STUB1. Initially, we performed interaction analyses between CDK9 and STUB1 when they are ectopically co-expressed within mammalian cells. As shown in Fig. 1E, ectopically expressed CDK9 showed strong interaction with ectopic STUB1 (lane 4). Further, to address this interaction directly in our in vitro reaction set up, we purified both CDK9 as well as STUB1 through their overexpression within mammalian cells and subsequent purification in high salt buffer condition to remove presence of other interacting proteins (Fig. 1F).[35] Subsequent in vitro interaction analyses clearly showed CDK9 interaction with STUB1 (Fig. 1G, lane 4). Based on all these results, we conclude that human CDK9 shows novel interaction with STUB1 within mammalian cells and that, this interaction is specific to

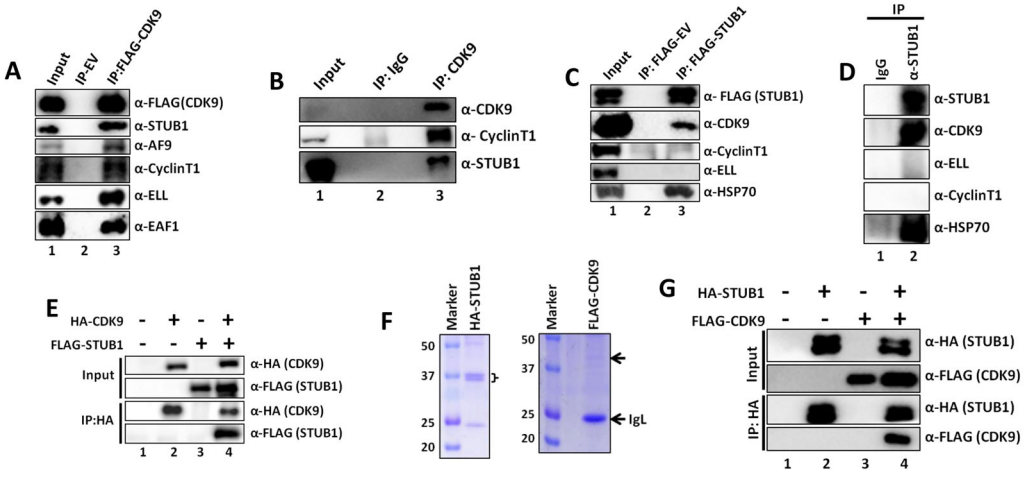

FIG 1 STUB1 is a novel interactor of CDK9. (A) Immunoprecipitation and subsequent Western blotting analysis showing interaction of ectopically-expressed FLAG-CDK9 with endogenous STUB1 along with its other known interactors within 293T cells. (B) Immunoprecipitation of endogenous CDK9 using specific antibody and subsequent Western blotting analysis showing interaction of STUB1 along with CyclinT1 with endogenous CDK9 within 293T cells. (C) Immunoprecipitation and subsequent Western blotting analysis showing interaction of ectopically-expressed FLAG-STUB1 with endogenous CDK9 along with its other known interactor HSP70 within 293T cells. STUB1 fails to show interaction with other CDK9-interacting proteins such as CyclinT1 and ELL. (D) Immunoprecipitation of endogenous STUB1 using specific antibody and subsequent Western blotting analysis showing interaction of CDK9 along with HSP70 with endogenous STUB1 within 293T cells. STUB1 also fails to show interaction with other CDK9-interacting proteins such as CyclinT1 and ELL in endogenous context as well. (E) Co-immunoprecipitation and subsequent Western blotting analysis showing interaction of ectopically expressed CDK9 with that of co-expressed STUB1 within 293T cells. (F) Coomassie staining showing purification of CDK9 and STUB1 through their overexpression within 293T cells and subsequent purification in high salt buffer condition. These purified proteins were used in direct interaction analyses as shown in next (G). (G) In vitro interaction analysis with purified proteins (F) showing direct interaction between STUB1 and CDK9 without the requirement of other interacting proteins.

the CDK9 component of the P-TEFb complex only. Further, and consistent with our conclusion that STUB1 only interacts with CDK9 component alone, immunoprecipitation of several ectopically expressed SEC components including ELL, AFF1, and AF9 failed to show their interaction with STUB1, whereas, same assay showed interaction of these components with their known interacting partners within the SEC complex (Fig. S1B to D).

CDK9 is subjected to ubiquitin proteasome-mediated degradation within mammalian cells. Since human STUB1 has been described as ubiquitin E3 ligase for regulation of multiple proteins through regulation of their stability, we surmised that in a similar manner, functions of CDK9 and thus P-TEFb complex within mammalian cells would also be regulated by STUB1. Functions of human P-TEFb complex have been well established in positive regulation of transcription in association with multiple factors including BRD4, SEC components, c-MYC, p53, as well as ZMYND8.[3,8–10,36] However, functional regulation of P-TEFb complex through regulation of its overall stability within mammalian cells have been poorly studied. With the exception of two studies that showed CyclinT1 interaction-dependent ubiquitination of CDK9 by SKP2-containing SCF Cullin E3 ubiquitin ligase complex,[13,14] no other studies reported detailed mechanisms of CDK9 ubiquitination including presence of other potential ubiquitin E3 ligase(s) as well as target residues being involved in this overall regulation. In an effort toward further understanding of functional regulation of P-TEFb complex within mammalian cells potentially by novel ubiquitin E3 ligase STUB1, we initially addressed whether human CDK9 protein would be subjected to ubiquitin proteasome-mediated degradation. We ectopically expressed CDK9 protein within 293T cells and addressed its stability by cycloheximide (CHX) chase assay. As shown in Fig. S2A (top panel for immunoblots and bottom panel for quantification), ectopically-expressed CDK9 showed half-life ($t_{1/2}$) of ~1 h. To address the similar question in endogenous context, CHX chase assay of endogenous CDK9 showed degradation kinetics with longer half-life than the ectopically expressed CDK9 ($t_{1/2}$ ~4hrs) (Fig. S2B, top panel for immunoblots and bottom panel for quantification). Toward addressing potential involvement of ubiquitin proteasome system for CDK9 degradation, we treated the cells with MG132 that inhibits the functions of ubiquitin proteasome system. As shown in Fig. S2C, CDK9 protein level is indeed regulated by ubiquitin proteasome-mediated degradation since addition of increasing concentration of MG132 progressively increased the endogenous CDK9 protein level. Consistent with a role of ubiquitin proteasome system in regulating CDK9 degradation, concomitant ectopic expression of ubiquitin from a plasmid, degraded ectopically expressed CDK9 as shown in Fig. S2D (lane 2 vs lanes 4–6). Immunoprecipitation of this ectopically expressed CDK9 further showed enhanced polyubiquitination when immunoblotted using ubiquitin-specific antibody. All these data clearly suggest that human CDK9 is subjected to ubiquitin proteasome-mediated degradation within mammalian cells.

Domain analysis of CDK9 and STUB1 for their interaction. For deeper understanding of molecular interactions between CDK9 and STUB1 and their implications in overall functional regulation, we subsequently addressed specific domains of these proteins that are required for their interaction within mammalian cells. We generated several CDK9- and STUB1-expressing plasmid constructs for their expression within mammalian cells based on their functional domains as shown Fig. 2A and C. Our initial analyses with various CDK9 deletion constructs showed that while a deletion of C-terminal end (277–372) did not impact overall CDK9 interaction with endogenous STUB1, a deletion of N-terminal region between 32 and 66 amino acids (67–276) markedly impaired this interaction (Fig. 2B, lane 5). Further deletion from 67–100 amino acids almost abolished CDK9 interaction with endogenous STUB1 (Fig. 2B, lanes 6–7). Thus, these domain analyses showed that human STUB1 interacts with the N-terminal region of CDK9 preferentially involving 32–100 amino acids of the N-terminal end.

STUB1 possesses several important domains in which the C-terminal U-box domain is primarily involved in ubiquitination of target proteins.[15] Further, the N-terminal tetratricopeptide repeat 1, 2 and 3 (TPR-1, 2 and 3) domains are involved in multiple

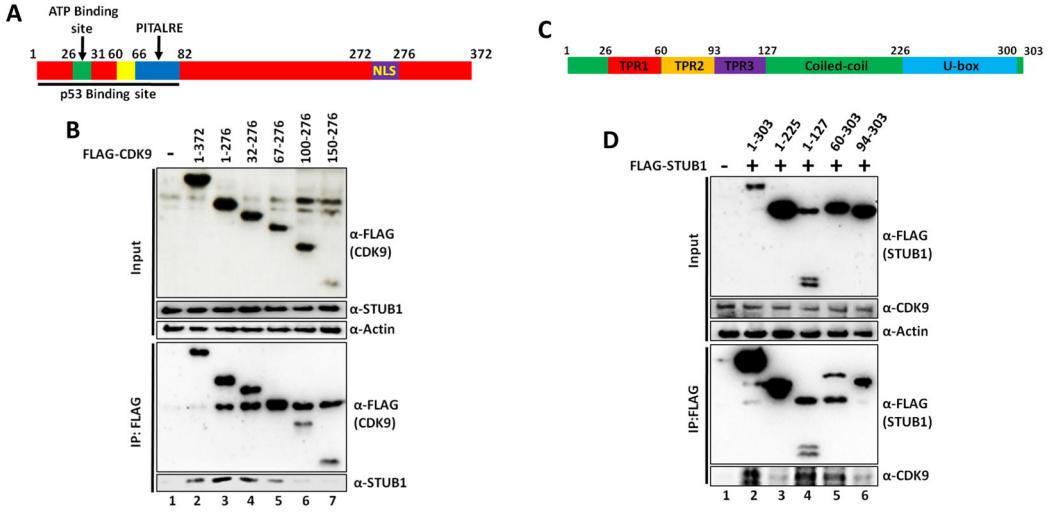

FIG 2 Domain analysis of CDK9 and STUB1 for their interaction within mammalian cells. (A) Cartoon diagram showing important domains present within CDK9 protein. (B) Immunoblotting showing domain analysis using plasmids expressing CDK9 domains as indicated, to identify their interaction with endogenous STUB1. Plasmids expressing indicated FLAG-CDK9 domains were expressed in 293T cells and these CDK9 fragments were immunoprecipitated using FLAG-antibody coated M2 agarose beads. Subsequent Western blotting was performed for identifying interaction with endogenous STUB1. (C) Cartoon diagram showing important domains present within STUB1 protein. (D) Immunoblotting showing domain analysis using plasmids expressing STUB1 domains as indicated, to identify their interaction with endogenous CDK9. Plasmids expressing indicated FLAG-STUB1 fragments were expressed in 293T cells and these STUB1 fragments were immunoprecipitated using FLAG-antibody coated M2 agarose beads. Subsequent Western blotting was performed for identifying interaction with endogenous CDK9.

protein-protein interactions. Toward addressing the specific domain within STUB1 that would be involved in its interaction with CDK9, we generated several STUB1 deletion fragments from both N- and C-terminal ends (Fig. 2C and D). Transfection of 293 T cells with these plasmid constructs and subsequent immunoprecipitation analyses showed that a fragment (1–225) that loses U-box, also shows its impaired interaction with endogenous CDK9 when compared to full-length STUB1 (Fig. 2D, compare lane 2 vs lane 3). However, interestingly, further deletion of the coiled-coil domain restored this interaction (Fig. 2D, lane 4). This observation suggests existence of two important domains within STUB1 for its interaction with CDK9, the C-terminal U-box as well as N-terminal TPR domains. Consistent with this hypothesis, a deletion fragment that looses the N-terminal TPR1 domain did not show marked effect on overall STUB1 and CDK9 interaction (Fig. 2D, lane 5). However, further deletion of TPR2 strongly reduced this interaction (Fig. 2D, lane 6). From all these interaction analyses, we conclude that while the STUB1 interacts with CDK9 with two functionally important domains i.e. C-terminal U-box and N-terminal TPR1-2, the internal coiled-coiled domain negatively regulates TPR-mediated CDK9 interaction in absence of critically important C-terminal U-box domain.

STUB1 promotes CDK9 degradation through ubiquitination within mammalian cells. Since our initial analyses indicated a role of ubiquitin proteasome system in regulation of CDK9 stability and our observation of strong interaction between CDK9 and STUB1 (Fig. S1 and Fig. 1 respectively), we hypothesized that human STUB1 may have a functional role in regulating CDK9 stability within mammalian cells involving its ubiquitin E3 ligase function present within the C-terminal U-box (Fig. 2C). Toward addressing this possibility, we cotransfected 293T cells with plasmids expressing CDK9 with increasing concentrations of STUB1 plasmid. As shown in Fig. 3A, with increasing expression of STUB1, expression of ectopically expressed CDK9 protein level goes down (compare lane 2 vs lanes 4–6). However, similar analysis failed to show any effect of STUB1 on the expression of ectopically expressed BRD4 (Fig. S3A), suggesting the specificity of STUB1 effect on CDK9 for its degradation. Further, overexpression of STUB1 reduced expression of endogenous CDK9 as well (Fig. 3B, compare lane 1 vs lanes 2–4). This effect is specific to CDK9 only, since, in the same assay, we have failed to observe any effect of overexpression of STUB1 on the expression of endogenous

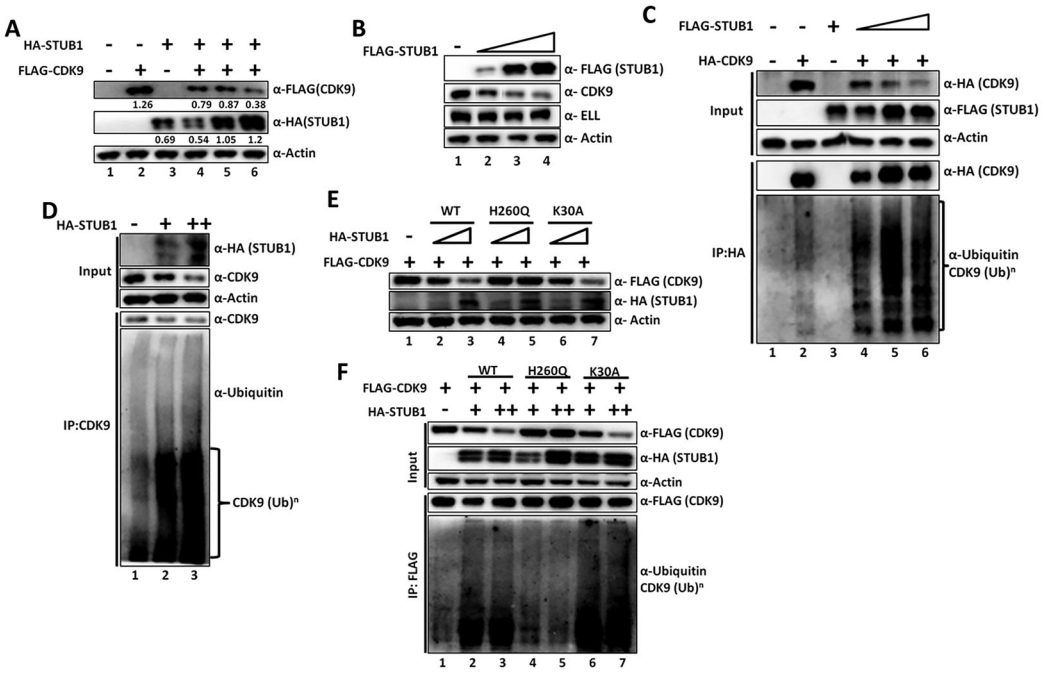

FIG 3 Hsc70 interaction-independent CDK9 degradation by STUB1 involving ubiquitin proteasome system. (A) Immunoblotting analysis showing degradation of ectopically-expressed CDK9 by overexpression of STUB1 within mammalian 293T cells. The quantification shows amount of corresponding protein level with respect to loading control actin. (B) Immunoblotting analysis showing degradation of endogenous CDK9 by overexpression of STUB1 within mammalian 293T cells. (C) Immunoblotting analysis showing enhanced ubiquitination of ectopically expressed CDK9 in presence of overexpressed STUB1 within mammalian 293T cells. (D) Immunoblotting analysis showing enhanced ubiquitination endogenous CDK9 in presence of overexpressed STUB1 within mammalian 293T cells. CDK9 was immunoprecipitated by using specific antibody. (E) Immunoblotting analysis showing degradation of ectopically expressed CDK9 by overexpression of WT and different mutants of STUB1 within mammalian 293T cells. The H260Q mutant represents catalytic-dead mutant at the U-box of STUB1 and the K30A represents Hsc70-interaction deficient mutant. (F) Immunoblotting analysis showing ubiquitination of ectopic CDK9 by overexpression of WT and different mutants of STUB1, as indicated, within mammalian 293T cells. In all of our immunoblotting assays in this figure, level of actin was used as loading control.

ELL protein (Fig. 3B). Consistent with a role of STUB1 in degrading target substrates through polyubiquitination, STUB1-mediated CDK9 degradation can be rescued through treatment of cells with MG132 that inhibits ubiquitin proteasome-mediated degradation (Fig. S3B). Overexpression of STUB1 in colorectal carcinoma cells HCT116, also showed its similar effect in degrading endogenous CDK9 without showing an effect on ELL (Fig. S3C). Thus, these results suggest that human STUB1 regulates CDK9 protein level within mammalian cells in a cell type-independent manner. Further, we also tested the specificity of STUB1-mediated degradation of CDK9 to other CDKs such as CDK7 and CDK8, that play key roles in transcriptional regulation. Interestingly, the overall effect of STUB1 in degradation of CDK9 is very specific since in the same assay, it failed to degrade both the CDK7 and CDK8 (Fig. S3D, compare lanes 2–4 with lanes 5–7 and 8–10). Further, the STUB1 also failed to show any interaction with CDK7 or CDK8 in our co-immunoprecipitation analyses, whereas, the same assay showed its interaction with CDK9 (Fig. S3E, compare lane 4 vs lanes 5 and 6). Thus, all these clearly indicated that the overall effect of STUB1 is very specific to the CDK9 component of P-TEFb complex and not to other transcriptionally important CDKs such as CDK7 and CDK8.

Next, to address a potential role of STUB1 in regulating CDK9 level through polyubiquitination, immunoprecipitation of ectopically expressed CDK9 showed strong polyubiquitination when co-expressed with STUB1 and immunoblotted with ubiquitin-specific antibody (Fig. 3C, compare lane 2 vs lanes 4-6). Over-expression of STUB1 and subsequent immunoprecipitation of endogenous CDK9 with specific antibody further confirmed polyubiquitination of endogenous CDK9 as well by STUB1 (Fig. 3D, compare lane 1 vs lanes 2–3). Thus, our results show that human STUB1 negatively regulates

CDK9 protein expression through promoting its polyubiquitination and subsequent degradation by ubiquitin proteasome system within mammalian cells.

STUB1 regulates CDK9 protein degradation in Hsc70-independent manner. Since STUB1 also functions as a co-chaperone through its interaction with Hsc70 for degradation of misfolded proteins,[15] we wondered whether the degradation potential of STUB1 for CDK9 within mammalian cells would be dependent on its interaction with Hsc70. Towards addressing that, we generated a STUB1 point mutation at the N-terminus (K30A) that loses its interaction with Hsc70.[17] Further, we also generated a STUB1 catalytic dead mutant in the U-box domain (H260Q) as a control in the same experimental setup.[17] As shown in Fig. 3E, whereas, the Hsc70 interaction-deficient STUB1 mutant (K30A) showed similar degradation potential as that of wild type (WT) (compare lane 1 vs lanes 2–3 and lane 1 vs lanes 6–7), the H260Q mutant failed to degrade CDK9 (compare lane 1 vs lanes 2–3 and lane 1 vs lanes 4–5). Subsequent immunoprecipitation and blotting analysis using ubiquitin-specific antibody clearly showed similar polyubiquitination potential of K30A STUB1 mutant to that of WT (Fig. 3F, compare lanes 2–3 vs lanes 6–7). However, the catalytic dead mutant of STUB1 (H260Q), failed to show any effect on CDK9 polyubiquitination in our assay (Fig. 3F, compare lanes 2–3 vs lanes 4–5). Therefore, based on all these evidences, we conclude that human STUB1 regulates CDK9 level within mammalian cells that is independent of its interaction with Hsc70.

STUB1 regulates CDK9 degradation kinetics within mammalian cells. Once established a role for STUB1 in CDK9 polyubiquitination and consequent degradation within mammalian cells, we wanted to address whether STUB1 can modulate the degradation kinetics of CDK9 when the level of its expression is regulated. We initially tested the effect of overexpression of STUB1 on degradation kinetics of ectopically expressed CDK9. As shown in Fig. 4A, concomitant overexpression of STUB1 markedly enhanced degradation kinetics (bottom panel) of ectopically expressed CDK9 (top panel for immunoblots, compare lanes 1–6 vs lanes 7–12). Overexpression of STUB1 also enhanced degradation kinetics of endogenous CDK9 as well (Fig. 4B, top panel for immunoblots, compare lanes 1–6 vs lanes 7–12 and bottom panel for quantification).

Next, for addressing a similar question when STUB1 expression is downregulated, we generated stable STUB1 knockdown cells using multiple shRNAs (Fig. 4C). Using these knockdown cells, CHX chase assays further showed reduced CDK9 degradation kinetics when STUB1 expression is downregulated by multiple shRNAs (Fig. 4D, top panel for immunoblots, compare CDK9 degradation kinetics between control scrambled (Scr) cells vs sh-STUB1 cells and bottom panel for quantification). All these experiments clearly showed a role for human STUB1 in regulation of CDK9 degradation within mammalian cells.

N-terminal lysine 3 (K3) residue of CDK9 is critically targeted for STUB1-mediated degradation within mammalian cells. For detailed understanding of the STUB1-mediated CDK9 degradation, we next addressed the critical residue(s) of CDK9 that would be targeted for STUB1-mediated ubiquitination and subsequent degradation within mammalian cells. In our initial assays, we used various CDK9 deletion constructs and co-expressed them with STUB1 to identify the specific domain that would be targeted for degradation. As shown in Fig. 5A, while the deletion of C-terminal 277–372 had little effect on STUB1-mediated CDK9 degradation (compare lanes 1–2 vs lanes 3–4), a deletion of N-terminal 31 amino acids markedly abrogated overall STUB1-mediated degradation (compare lanes 1–2 vs lanes 5–6). Further deletion from N-terminal end showed similar results of STUB1-mediated degradation. Thus, based on these domain analyses, we conclude that the human STUB1 targets residues within the N-terminal 31 amino acids for CDK9 degradation within mammalian cells.

Next, for identifying specific lysine residue(s) within the N-terminal domain that would be targeted for STUB1-mediated ubiquitination and subsequent degradation, we generated several CDK9 point mutants in combination of various lysine residues as shown in Fig. 5B. We also targeted few residues beyond N-terminal 31 amino acids to address the effect of introduction of mutations in adjacent lysine residues into this

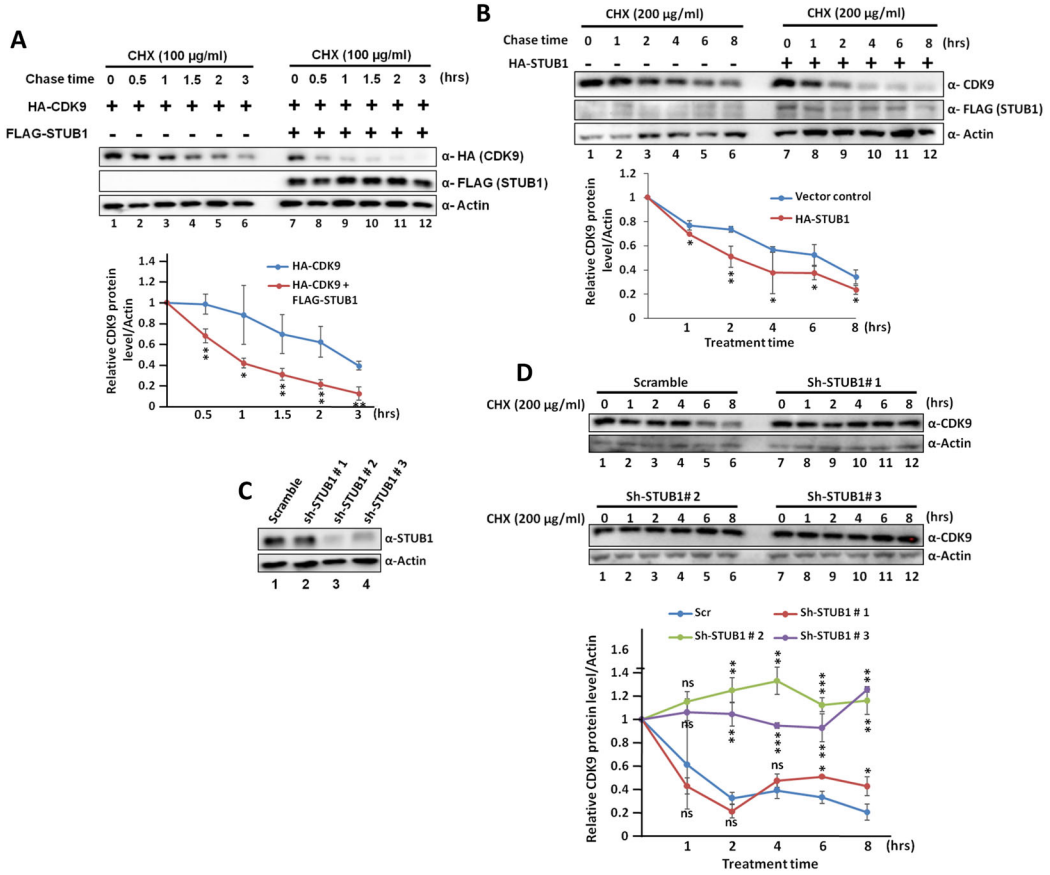

FIG 4 Overexpression and knockdown of STUB1 enhances and reduces CDK9 degradation respectively within mammalian cells. (A) Immunoblotting analysis showing cycloheximide (CHX) chase assay of degradation kinetics of ectopically expressed CDK9 in presence of ectopic STUB1 within 293T cells (top panel). Quantification of degradation kinetics as obtained from multiple biological and technical repeats are shown in the bottom panel. (B) Immunoblotting analysis showing CHX chase assay of degradation kinetics of endogenous CDK9 in presence of ectopic STUB1 within 293T cells (top panel). Quantification of degradation kinetics as obtained from multiple biological and technical repeats are shown in the bottom panel. (C) Immunoblotting analysis showing stable knockdown of STUB1 by multiple shRNAs within 293T cells. (D) Immunoblotting analysis showing CHX chase assay of degradation kinetics of endogenous CDK9 upon knockdown of STUB1 by multiple shRNAs within 293T cells (top panel). Quantification of degradation kinetics as obtained from multiple biological and technical repeats are shown in the bottom panel. In all of our immunoblotting assays in this figure, level of actin was used as loading control. In these analyses as shown in the figure, data represents mean ± S.D. One-tailed Student's *t* test was used to calculate the statistical significance of the data in this figure. $^{*}P \leq 0.05$, $^{**}P \leq 0.01$, $^{***}P \leq 0.001$, and ns denotes not significant. At least n = 2 biological replicates were performed for each experiment.

overall regulation. Interestingly, introducing mutations of lysine residues within the N-terminal 31 amino acids showed clear resistance against STUB1-mediated degradation (Fig. 5B, compare lanes 1–3 vs lanes 4–6), whereas mutations in other lysine residues had little effect on STUB1-mediated degradation. These results of mutational analysis are also consistent with our domain analysis as shown in Fig. 5A. Introduction of further mutations showed that a single point mutation at lysine 3 residue (K3A) of CDK9 caused complete resistance against STUB1-mediated degradation (Fig. 5C, compare lanes 1–3 vs lanes 4–6), while other lysine mutations had minimal effect (Fig. 5C, compare lanes 1–3 vs lanes 7–9). Thus, we conclude that the N-terminal lysine 3 (K3) residue within CDK9 is critically being targeted for STUB1-mediated degradation within mammalian cells.

To further address whether the K3 residue of CDK9 is being targeted for STUB1-mediated polyubiquitination and thus causes its degradation, we cotransfected WT and K3A-expressing CDK9 plasmid constructs along with STUB1. As shown in Fig. 5D, and consistent with our data as shown in Fig. 5C, we also observed resistance against STUB1-mediated degradation by K3A mutant as compared to WT CDK9 (input panel, compare lanes 2–3 vs 5–6). Subsequent immunoprecipitation and blotting analysis using ubiquitin-specific antibody clearly showed enhanced polyubiquitination of WT

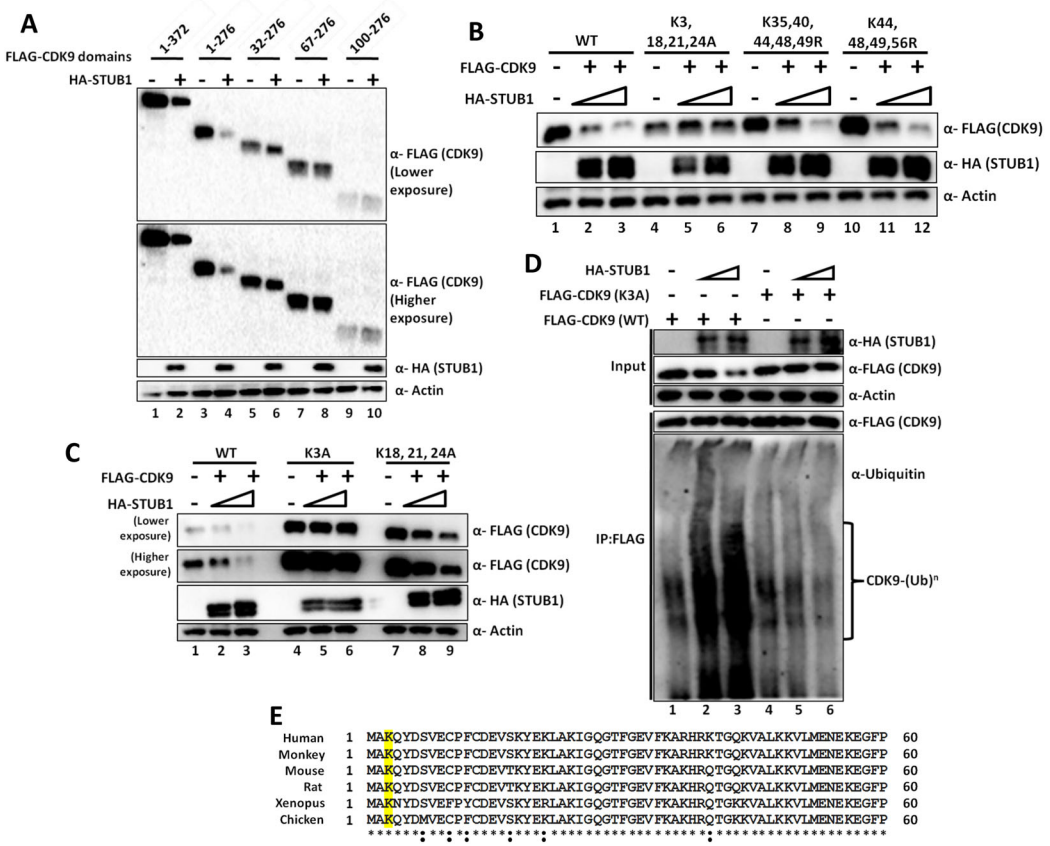

FIG 5 N-terminal lysine3 (K3) residue of CDK9 is critically targeted by STUB1 for ubiquitin proteasome-mediated degradation within mammalian cells. (A) Immunoblotting analysis showing domain analysis using plasmids expressing indicated CDK9 fragments for identifying specific regions within CDK9 that would be targeted for STUB1-mediated degradation within mammalian cells. (B) Immunoblotting analysis showing mutation analysis using plasmids expressing indicated CDK9 mutants for identifying specific combination of mutations within CDK9 that would show resistance to STUB1-mediated degradation within mammalian cells. (C) Immunoblotting analysis showing further mutation analysis using plasmids expressing indicated CDK9 mutants for identifying lysine 3 (K3) as the key target for STUB1-mediated degradation since K3A mutant showed complete resistance against STUB1-mediated degradation within 293T cells. (D) Immunoblotting analysis showing markedly reduced presence of ubiquitination of CDK9 (K3A) mutant when compared to wild-type (WT) in presence of overexpressed STUB1 within 293T cells. Ectopically expressed CDK9 was immunoprecipitated using FLAG antibody-coated M2 agarose beads and presence of ubiquitination was assessed by immunoblotting analysis using ubiquitin-specific antibody. (E) Multiple sequence alignment showing conserved nature of CDK9 K3 residue across multiple species as indicated. In all of our immunoblotting assays in this figure, level of actin was used as loading control.

CDK9 in presence of STUB1 (Fig. 5D, compare lane 1 vs lanes 2–3). However, in the same assay, the K3A mutant of CDK9 failed to show any enhanced polyubiquitination in presence of STUB1 (Fig. 5D, compare lane 4 vs lanes 5–6). Consistent with a role for K3 polyubiquitination in maintenance of CDK9 level, three earlier high throughput analyses showed presence of K3 ubiquitination within mammalian cells when grown under normal conditions.[37–39] However, these studies failed to provide any details of potential cognate E3 ligase(s) that could play essential role in overall regulation. Further, consistent with a key role of this lysine residue in overall functional regulation, we have observed sequence conservation of this K3 residue of CDK9 across multiple species that we have analyzed (Fig. 5E). This sequence conservation further suggests importance of this residue in overall functional regulation. Thus, based on all these analyses, we conclude that human CDK9 is subjected to STUB1-mediated degradation within mammalian cells through ubiquitination of a conserved N-terminal lysine 3 residue.

CyclinT1 competes with STUB1 for binding at N-terminus and thus stabilizes CDK9. Since the cognate CDK9-associated cyclin, CyclinT1 also interacts with the N-terminal end of CDK9,[34] we surmised that by doing so, CyclinT1 could protect CDK9 from being degraded by STUB1 upon its binding. In our initial analyses, concomitant expression of CyclinT1 reversed the STUB1-mediated degradation of ectopic CDK9 within

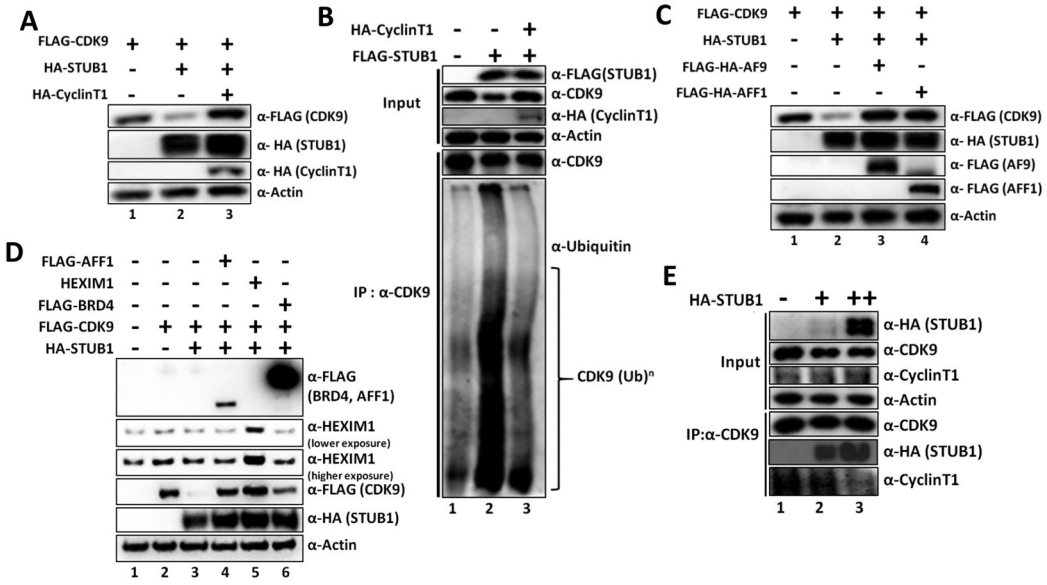

FIG 6 CyclinT1 protects CDK9 from STUB1-mediated degradation. (A) Immunoblotting analysis showing effect of overexpression of CyclinT1 on STUB1-mediated degradation of ectopic CDK9 within 293T cells. (B) Immunoblotting analysis showing effect of overexpression of CyclinT1 on STUB1-mediated ubiquitination and degradation of endogenous CDK9 within 293T cells. Endogenous CDK9 was immunoprecipitated using specific antibody and presence of ubiquitination was assessed by immunoblotting using ubiquitin-specific antibody. (C) Immunoblotting analysis showing effect of overexpression of AF9 and AFF1 on STUB1-mediated degradation of ectopic CDK9 within 293T cells. (D) Immunoblotting analysis showing effect of overexpression of BRD4 and HEXIM1 on STUB1-mediated degradation of ectopic CDK9 within 293T cells. (E) Immunoblotting analysis showing competition between CyclinT1 and STUB1 for their binding to endogenous CDK9 within 293T cells. In presence of increased expression of STUB1 and its binding, concomitant reduction of binding of endogenous CyclinT1 is observed. In all of our immunoblotting assays in this figure, level of actin was used as loading control.

mammalian cells (Fig. 6A, compare lane 2 vs lane 3).We also observed a similar phenomenon, wherein, ectopic overexpression of CyclinT1 rescued STUB1-mediated degradation of endogenous CDK9 as well (Fig. 6B, input panel, compare lane 2 vs lane 3). Subsequent immunoprecipitation of endogenous CDK9 by using specific antibody clearly showed enhanced polyubiquitination upon ectopic overexpression of STUB1 that correlated with its degradation as observed (Fig. 6B, compare lane 1 vs lane 2). Interestingly, and consistent with its effect on stabilization, we observed reduced polyubiquitination of endogenous CDK9 by STUB1 upon concomitant overexpression of CyclinT1 (Fig. 6B, compare lane 2 vs lane 3). These data clearly indicate a role for CyclinT1 in protecting CDK9 against STUB1-mediated degradation within mammalian cells. Our further analyses showed that factors that directly interacts with CyclinT1 and help in assembly of SEC,[10] also showed similar protection against STUB1-mediated degradation of CDK9 when they are co-expressed within mammalian cells (Fig. 6C). Further, similar protection is also observed when we co-expressed other P-TEFb-interacting proteins such as BRD4 and HEXIM1 (Fig. 6D). Thus, based on all these analyses, we conclude that human CyclinT1 and its associated factors protect CDK9 against STUB1-mediated degradation within mammalian cells.

Further, we also addressed the mechanism of CyclinT1 in overall protection of CDK9 from STUB1-mediated degradation. We hypothesized that, through its binding at N-terminus, CyclinT1 could exclude STUB1 binding to CDK9 since similar region is also involved in CDK9 interaction with STUB1 (Fig. 2B). As shown in Fig. 6E, increasing ectopic expression of STUB1 and its binding leads to reduced CyclinT1 interaction with endogenous CDK9 (compare lane 1 vs lanes 2–3). Thus, binding of CyclinT1 at the N-terminal end of CDK9 protects it from STUB1-mediated degradation by (a) reducing concomitant STUB1 binding and (b) reducing subsequent K3 polyubiquitination and degradation.

Knockdown of STUB1 increases expression of diverse P-TEFb-target genes within mammalian cells. Since overexpression of STUB1 reduced endogenous CDK9 level (Fig. 3B and Fig. S3B), we wondered whether its knockdown would enhance

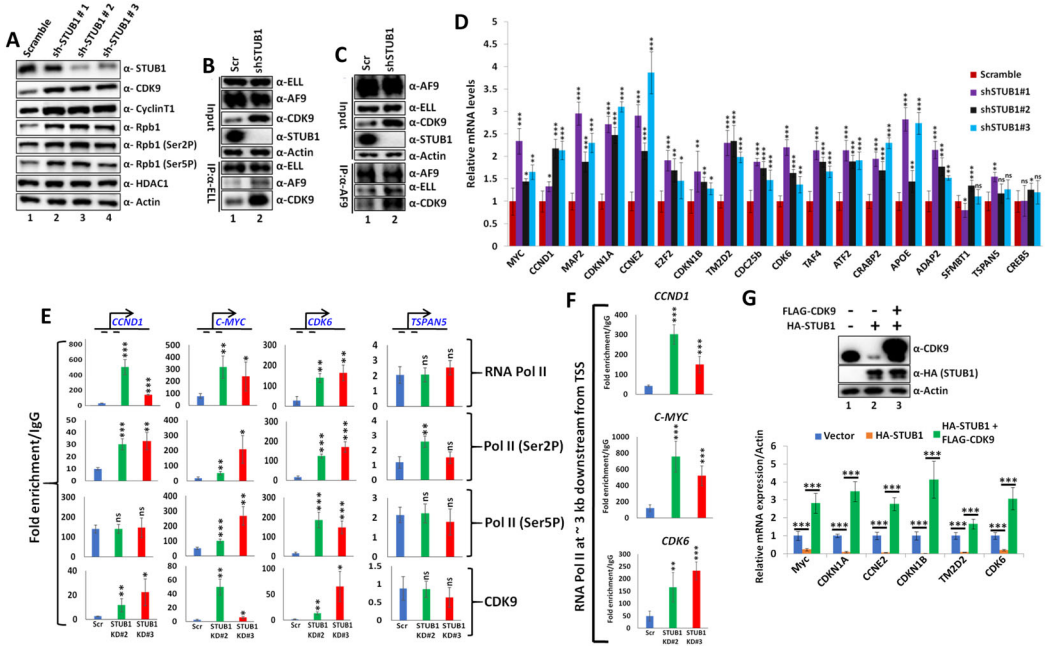

FIG 7 Knockdown of STUB1 enhances CDK9 expression and thus increases P-TEFb recruitment on target genes resulting in their increased expression. (A) Immunoblotting analysis showing effect of STUB1 knockdown on expression of CDK9 and other factors as indicated. Enhanced expression of CDK9 also shows concomitant increased expression of CyclinT1 resulting in increased level of global Pol II Ser2 and Ser5 phosphorylation within mammalian 293T cells. (B) Immunoblotting analysis showing enhanced association of endogenous CDK9 with ELL-associated SEC, when immunoprecipitated with specific antibody, upon STUB1 knockdown in 293T cells. (C) Immunoblotting analysis showing enhanced association of endogenous CDK9 with AF9-associated SEC, when immunoprecipitated with specific antibody, upon STUB1 knockdown in 293T cells. (D) qRT-PCR analysis showing effect of STUB1 knockdown by multiple shRNA constructs on mRNA expression of indicated target genes. The level of each target mRNA was normalized with Actin. (E) ChIP and subsequent qRT-PCR analysis showing indicated factor recruitment at promoter proximal region of the indicated target genes upon STUB1 knockdown by two different shRNA constructs. Scramble (Scr) knockdown was used as control in our experiment. (F) ChIP and subsequent qRT-PCR analysis showing Pol II recruitment at ~3 kb downstream region from transcription start site (TSS) of the indicated target genes upon STUB1 knockdown by two different shRNA constructs. Scramble (Scr) knockdown was used as control in our experiment. (G) Immunoblotting analyses showing re-expression of CDK9 in the STUB1 overexpressed cells (top panel). Overexpression of STUB1 reduces endogenous CDK9 protein level. However, through overexpression, the overall level of CDK9 protein is restored. Analysis of mRNA expression of the target genes as indicated in the cells expressing the target proteins as indicated (bottom panel). In our mRNA expression as well as ChIP analyses as shown in this figure, qRT-PCR data represents mean ± S.D. One-tailed Student's *t* test was used to calculate the statistical significance of the data in this figure. $^{*}P \leq 0.05$, $^{**}P \leq 0.01$, $^{***}P \leq 0.001$, and ns denotes not significant. At least n = 2 biological replicates were performed for each experiment. In all of our immunoblotting assays in this figure, level of actin was used as loading control.

CDK9 level and thus functionally regulate P-TEFb-mediated target gene expression within mammalian cells. To address this, we used shRNA-mediated stable STUB1 knockdown in 293T cells (Fig. 4C) for our subsequent analyses. Our initial analyses showed that STUB1 knockdown enhances expression of endogenous CDK9 in all three shRNA constructs that we have used (Fig. 7A, compare lane 1 vs lanes 2–4). Notably, along with CDK9, we also observed increased expression of CyclinT1, potentially through cooperative stabilization effect of CDK9 to CyclinT1 in functional P-TEFb complex. Along with enhanced expression of P-TEFb complex, we also observed enhanced level of global Pol II CTD phosphorylation at Ser2 and Ser5 residues of heptad repeat since P-TEFb complex has been shown to target these two residues for their phosphorylation. Further, consistent with an earlier study showing a role of CTD Ser5 phosphorylation in stabilizing Pol II against ubiquitin E3 ligase Def1-mediated degradation,[40] we also observed enhanced level of total Pol II upon knockdown of STUB1 that also resulted in increased CTD Ser5 phosphorylation (Fig. S4A for quantification). To address the cell type specificity of overall effect of modulation of STUB1 expression on CDK9 protein level within mammalian cells, we used HCT116 cells for our subsequent assays. Our initial analyses of overexpression of STUB1 showed reduced CDK9 expression along with concomitant reduced global level of Ser2 and Ser5 phosphorylation of Pol II CTD in HCT116 cells as well (Fig. S4B, compare lane 1 vs lanes 2–3). In a subsequent analysis, knockdown of STUB1 showed markedly enhanced Ser2 and Ser5 phosphorylation of Pol II CTD (Figs. S4C, compare lane 1 vs lanes 2–3 and S4D for quantification).

Interestingly, enhanced CTD Ser5 phosphorylation also resulted in increased expression of Pol II in this cell line. Thus, based on all these observations, we conclude that human STUB1 regulates global level of Pol II CTD phosphorylation at Ser2 and Ser5 residues through regulation of overall level of CDK9 and thus P-TEFb complex formation within mammalian cells. The effect of STUB1 in regulating CDK9 level and thus P-TEFb complex is cell type independent.

Enhanced CDK9 association within SEC upon STUB1 knockdown. Our observation of enhanced CDK9 expression leading to global increase in Pol II CTD Ser2 and Ser5 phosphorylation suggested that upon STUB1 knockdown, enhanced association of CDK9 within SEC could lead to this observation. For addressing this hypothesis, we immunoprecipitated SEC through endogenous ELL using specific antibody and tested CDK9 association in this immunoprecipitated sample. As shown in Fig. 7B, when compared to control (Scr), STUB1 knockdown showed markedly enhanced association of CDK9 with this ELL-associated SEC. Interestingly, along with CDK9, we also observed modest increase in AF9 association as well. Further, to substantiate the similar observation, we also immunoprecipitated SEC through endogenous AF9 using specific antibody. As shown in Fig. 7C, consistent with our observation with immunoprecipitation of ELL, AF9-associated SEC also showed enhanced presence of CDK9 as well upon STUB1 knockdown when compared to control Scr cells. These observations clearly showed that upon STUB1 knockdown, enhanced expression of CDK9 resulted in its enhanced association within SEC. This enhanced association provides the explanation for increased global level of Ser2 and Ser5 phosphorylation upon STUB1 knockdown within mammalian cells.

Knockdown of STUB1 increases expression of diverse sets of genes within mammalian cells. Since STUB1 knockdown enhanced global level of Ser2 and Ser5 phosphorylated form of Pol II, we envisaged that, by doing so, it can increase the expression of global P-TEFb-target genes. Towards identifying the specific genes, we focused on the target genes which predominantly have been shown to require functions of SEC by many of our studies in last few years.[3,34–42,43] We reasoned that since P-TEFb is a key component of SEC, its increased expression could lead to enhanced SEC functions resulting in increased target gene expression. As expected, knockdown of STUB1 showed increased mRNA expression of diverse target genes that we analyzed (Fig. 7D). The overall effect is specific since in the same assay, we failed to observe much effect on non-target genes such as *TSPAN5* and *CREB5*. The overall target genes include the ones that are involved in cell proliferation as well as well as glucose metabolism among others.

To further identify that these sets of genes are indeed the targets of P-TEFb-mediated expression, we performed a parallel analysis, in which, we over-expressed CDK9 component of P-TEFb complex within 293T cells and tested the overall effect on target gene expression. Overexpression of CDK9 markedly enhanced global level of Ser2 and Ser5 phosphorylated form of Pol II (Fig. S4E, compare lane 1 vs lane 2) similar to the one observed upon STUB1 knockdown (Fig. 7A). Increase in global Pol II Ser2 and Ser5 phosphorylation by overexpression of CDK9 also resulted in increased expression of most of the genes that we have tested for their enhanced expression upon STUB1 knockdown (Fig. S4F). Thus, by correlating these observations, we conclude that an enhanced expression of CDK9 upon STUB1 knockdown results in increased expression of majority of the P-TEFb target genes that we have tested within mammalian 293T cells.

Knockdown of STUB1 also enhances expression of P-TEFb target genes within colorectal carcinoma HCT116 cells. Since we have observed enhanced expression of diverse P-TEFb target genes upon STUB1 knockdown within 293T cells, we wondered whether this overall effect would be specific to cell types being used in our experimental setup. To address that, we used the stable STUB1 knockdown HCT116 cells as mentioned in Fig. S4C. Consistent with our observation in 293T cells, we also observed significant upregulation of similar sets of genes in the HCT116 cells as well upon STUB1 knockdown (Fig. S4G). Similar to our observation in 293T cells, the overall effect

of STUB1 knockdown in increasing target gene expression is specific since in HCT116 cells as well, we have not observed enhanced expression of non-target *TSPAN5* and *CREB5* genes. Based on all these observations, we conclude that human STUB1 negatively regulates expression of diverse target genes in a cell type-independent manner, by regulating the level of CDK9 protein through its ubiquitin E3 ligase function.

STUB1 knockdown enhances recruitment of P-TEFb at the promoter proximal region of target genes leading to enhanced CTD Ser2 and Ser5 phosphorylation. Since we have observed enhanced expression of target genes upon STUB1 knockdown that correlates with increased CDK9 level and global Pol II Ser2 and Ser5 phosphorylation, we addressed whether similar phenomenon would be observed on target genes as well upon increased CDK9 and thus, P-TEFb recruitment. We performed ChIP analysis for addressing target factor recruitment at the promoter proximal region using gene-specific primers. As a control of our experimental set up, we also performed similar analyses on non-target *TSPAN5* gene that failed to show enhanced expression upon STUB1 knockdown. As shown in Fig. 7E, knockdown of STUB1 by two different shRNAs showed enhanced recruitment of CDK9 at the promoter proximal region of target *CCND1*, *C-MYC* and *CDK6* genes. However, we failed to observe any enhanced binding of CDK9 on the non-target *TSPAN5* gene in our assay. Consistent with enhanced CDK9 recruitment and functions of P-TEFb, we have observed enhanced level of Pol II CTD Ser2 phosphorylation on all the target genes that we have tested. However, we have observed enhanced Ser5 phosphorylation on two of those target genes suggesting that the STUB1 knockdown may not have equal effect on Ser5 phosphorylation on all the target genes that show enhanced expression. Interestingly, along with increased Ser2 and Ser5 phosphorylation, we have also observed enhanced total amount of Pol II as well. This is not a result of increased pausing since we have observed enhanced Ser2 phosphorylation that leads to the release of paused Pol II from the promoter proximal region to the coding region marking the productive elongation step. Indeed, consistent with this hypothesis, we have observed significantly enhanced Pol II on the coding region (~3 kb downstream of TSS) of all the target genes that we have tested (Fig. 7F). This observation clearly indicated enhanced release of Pol II from the promoter proximal region to the coding region (Fig. 7E). The enhanced Pol II presence is thus a reflection of its increased recruitment for transcriptional activation of these target genes.

To show the overall effect of STUB1 on regulating expression of target genes within mammalian cells is indeed specific to P-TEFb only, we overexpressed CDK9 from a plasmid in cells in which CDK9 expression is reduced upon overexpression of STUB1 (Fig. 7G, top panel immunoblots). Interestingly, re-expression of CDK9 in STUB1 overexpressed cells completely restored defect in target gene expression (Fig. 7G, bottom panel RNA analysis). This analysis further confirmed the overall effect of STUB1 in regulating target gene expression in P-TEFb complex-specific manner.

Therefore, based on all these observations, we conclude that human STUB1 negatively regulates expression of diverse target genes through negative regulation of overall level of CDK9 and thus P-TEFb complex within mammalian cells through its ubiquitin E3 ligase function for overall functional regulation.

DISCUSSION

The major aim of our study is to identify a novel ubiquitin E3 ligase for the CDK9 component of P-TEFb complex for its functional regulation. Through its ubiquitin E3 ligase function, STUB1 regulates the level of cellular CDK9, and thus in turn the P-TEFb complex, to regulate the expression of its target genes within mammalian cells. A single key N-terminal lysine 3 (K3) of CDK9 is being targeted for STUB1-mediated polyubiquitination and subsequent ubiquitin proteasome-mediated degradation. By virtue of similar N-terminal region being involved in its interaction, CyclinT1 competes with STUB1 for its binding and protects the CDK9 from STUB1-mediated degradation. The factors that cooperatively bind with CyclinT1 in forming functionally important SEC, also protects CDK9 degradation by STUB1. Thus, through its functional regulation of

free CDK9 within mammalian cells, STUB1 regulates overall pool of P-TEFb complex formation and target gene expression. An overall model for this mechanism of action as deciphered in this study, is presented in Fig. S5.

Regulation of CDK9 protein level through ubiquitination. Although the P-TEFb complex was described a while ago, quite surprisingly, the regulation of CDK9 protein level in regulation of P-TEFb complex function in overall transcriptional regulation have not been described in detail. To our knowledge, only two studies have reported functional regulation of CDK9 through ubiquitination mediated by SCF^{SKP2}-Cullin ubiquitin E3 ligase complex.[13,14] Functions of P-TEFb complex have been widely studied especially its role in releasing the paused Pol II at the promoter proximal region. Therefore, mechanistic understanding of these functional regulations via multiple pathways would significantly enhance overall knowledge of transcriptional activation. Considering the widely acknowledged functional role of P-TEFb complex in transcriptional regulation, our study would significantly advance the overall understanding of P-TEFb-mediated target gene activation.

The majority of the CDK-cyclin pairs work during a specific stage of cell cycle. Activity of those cell cycle dependent CDKs are controlled significantly by the availability of their partner cyclins. Due to that reason cells produce a particular type of cyclin in one phase of cell cycle and degrades it when that phase is over. Although this phenomenon is true for most of the CDK-cyclin complexes, CDK9-cyclin T1 complex remains active throughout the cell cycle. Therefore, cells are required to maintain an optimum level of both CDK9 and CyclinT1 all the time. To maintain a steady state level of CDK9 cells use STUB1 as an ubiquitin E3 ligase to fine-tune the cellular level and activity of CDK9.

Lysine 3 (K3) residue-mediated regulation of CDK9 level by STUB1. Although two earlier studies pointed toward a role for SCF^{SKP2}-Cullin ubiquitin E3 ligase complex in regulation of CDK9 level in P-TEFb-mediated regulation of HIV promoter-dependent gene expression, they failed to identify the specific residue(s) that are being targeted for degradation by the reported ubiquitin E3 ligase complex. Our study, as shown here, clearly pointed toward a critical role of N-terminal lysine 3 (K3) residue in regulation of STUB1-mediated polyubiquitination and subsequent degradation since a CDK9 mutant at this lysine residue failed to show enhanced polyubiquitination of CDK9 upon concomitant overexpression of STUB1 (Fig. 5). Ubiquitination of CDK9 on this residue has been described by high throughput proteomics studies by earlier reports.[37–49] However, those reports failed to decipher functional significance of ubiquitination on this residue in overall regulation as well as detailed associated mechanisms. Thus, our study is the first of its kind to identify a specific residue within CDK9 that is being targeted for ubiquitination for its degradation.

However, a few other high throughput proteomic studies also showed presence of CDK9 ubiquitination in other lysine residues as well.[44,45] It could be possible that STUB1-mediated CDK9 degradation involves K3 residue, whereas, other potential unexplored ubiquitin E3 ligases could also play important roles in overall maintenance of CDK9 protein level involving other lysine residues within mammalian cells. Further studies would be required for identifying other potential ubiquitin E3 ligases in overall regulation. Nonetheless, our study would significantly advance our overall understanding of regulation of P-TEFb complex functions for target gene expression through regulation of stability of its key kinase subunit CDK9, involving polyubiquitination of N-terminal K3 residue by STUB1.

STUB1-mediated CDK9 polyubiquitination and degradation and corresponding protection through interacting proteins. In our earlier study, we showed that human CyclinT1 interacts with CDK9 through its N-terminal region.[34] Since STUB1 also targets the lysine residue within this region for degradation of CDK9, it is quite conceivable that CyclinT1, upon its binding to CDK9, may protect it from STUB1-mediated degradation. Indeed, our data shown in Fig. 6, confirms this hypothesis. Interestingly, along with CyclinT1, its other direct interaction partners within the SEC complex,[10] as well as BRD4 and HEXIM1 also stabilize the CDK9 from STUB1-mediated degradation. Thus,

based on our results, it seems that, STUB1 could potentially target CDK9 for its polyubiquitination and degradation only when it remains as free form. Consistent with this hypothesis, our results show that human STUB1 only interacts with CDK9 and not other components of SEC (Fig. 1). Thus, once a complex being formed, either as P-TEFb or associated with interacting partners in SEC, BRD4 or 7SK snRNA, CDK9 remains protected from STUB1-mediated degradation. However, suffice to say that, the regulation of free CDK9 level is also important in overall regulation of its association with CyclinT1 in P-TEFb complex formation. An enhanced expression of CDK9, upon STUB1 knockdown, enhances overall P-TEFb complex formation leading to increased level of global Pol II CTD phosphorylation that leads to increased expression of diverse target genes as shown in Fig. 7. Therefore, regulation of free pool of CDK9 is also an important criterion for maintaining an optimal level of P-TEFb complex for efficient regulation of target gene expression.

It is interesting to note that two different functional roles of CyclinT1 in regulation of the CDK9 protein level have been described. The earlier study reported a role for CyclinT1 in augmenting CDK9 ubiquitination involving SCF^{SKP2}-Cullin ubiquitin E3 ligase complex,[13] whereas, our study pointed toward its role in stabilization. These observations raise the possibility of differential functional role of CyclinT1 involving different ubiquitin E3 ligase complex in regulation of CDK9 protein stability within mammalian cells. It could also be possible that the SCF^{SKP2}-Cullin ubiquitin E3 ligase complex may target other lysine residue than the K3 as discussed for STUB1 in our study. Whether CyclinT1 would promote ubiquitination at lysine residues other than K3, would be an interesting question for future exploration.

STUB1 functions in transcriptional upregulation by regulating the stability of transcription factors. Several key transcription factors including c-MYC or disease-causing mutant p53 have been shown to be regulated by the STUB1-mediated degradation.[46] Besides these, analysis of reduced STUB1 expression in gastric cancer patients has been shown to strongly correlate with shorter life expectancies in part through STUB1-medaited degradation of NF-κB/p65 resulting in inhibition of IL-8 induced angiogenesis.[30] Thus, in majority of diseases, reduced expression of STUB1 has been linked with enhanced expression of multiple target genes that ultimately lead to pathogenesis. The enhanced expression of proteins upon reduced expression of STUB1 have predominantly been linked to its ubiquitin E3 ligase function. However, our results suggest a newer regulatory pathway, wherein, a reduced STUB1 could lead to enhanced formation of P-TEFb complex. The enhanced P-TEFb complex formation would in turn increase the expression of target genes at transcriptional level. Thus, the overall effect of reduced STUB1 expression in increasing expression of protein may not necessarily be a reflection of its impaired ubiquitin E3 ligase function, but could also be a result of increased transcription owing to the formation of enhanced P-TEFb complex for functional regulation. Thus, further studies would be required for deeper mechanistic understanding of role of each pathway, i.e. ubiquitin E3 ligase and enhanced P-TEFb complex formation, in overall enhanced expression of any target protein upon reduced expression of STUB1.

MATERIALS AND METHODS

Cell culture and transfection. All cell lines were cultured at 37 °C and 5% CO_2 in Dulbecco's modified Eagle's medium (DMEM) (Invitrogen, USA) with 10% FBS (Gibco, USA) and 100 U/mL penicillin-streptomycin (Life Technologies, USA). Transfections were done using FuGENE transfection reagent (Promega, USA) as per manufacturer's protocol. For transfection-based experiments, cells were harvested after 48 h post-transfection, unless mentioned otherwise.

Plasmids, primers, and antibodies. All the plasmids used in this study, primers used for cloning, RNA and ChIP analyses, shRNA constructs used for knocking down expression of target genes and antibodies used in this study are mentioned in Tables 1 to 6.

Generation of stable knockdown cell lines. Specific shRNAs were cloned into pLKO.1 vector for making stable knockdown cell lines. 375 ng of psPAX2 (packaging plasmid), 125 ng of pMD2.G VSV-G (envelope plasmid) and 500 ng of shRNA expressing plasmid were transfected in 293T cells in each well of a 6-well plate. Old media was replaced by fresh media after 24 h of transfection. 48 h after addition of fresh media, virus containing supernatant was collected and was used for transducing freshly seeded target cells at a confluency level of 40–50%. Polybrene (Sigma, USA) was added (8 μg/mL final

TABLE 1 List of plasmids used

Name of plasmid	Description	Source
M10	FLAG-HA pcDNA5-FRT-TO vector	10
M13	AF9 cloned into FLAG-HA pcDNA5-FRT-TO vector	10
M24	AFF1 cloned into FLAG-HA pcDNA5-FRT-TO vector	10
M250	CDK9 cloned into FLAG-HA pcDNA5-FRT-TO vector	3
M296	psPAX2 lentivirus packaging plasmid	Addgene plasmid #12260
M297	pMD2.G lentivirus envelope plasmid	Addgene plasmid #12259
M298	Lentiviral pLKO.1 vector containing scramble sequence (as a control for shRNA knockdown)	41
M447	FLAG pcDNA5-FRT-TO vector	Invitrogen
M448	HA pcDNA5-FRT-TO vector	Invitrogen
M484	BRD4(L) cloned into FLAG pcDNA5-FRT-TO vector	3
M619	CDK9 cloned into FLAG pcDNA5-FRT-TO vector	34
M620	CDK9 cloned into HA pcDNA5-FRT-TO vector	34
M747	ELL cloned into FLAG pcDNA5-FRT-TO vector	35
M912	Ubiquitin cloned into EGFP-C1 vector	Addgene plasmid #11928
M935	CDK9 (1-276) fragment cloned into FLAG pcDNA5-FRT-TO vector	34
M936	CDK9 (32-276) fragment cloned into FLAG pcDNA5-FRT-TO vector	34
M937	CDK9 (67-276) fragment cloned into FLAG pcDNA5-FRT-TO vector	34
M938	CDK9 (100-276) fragment cloned into FLAG pcDNA5-FRT-TO vector	34
M939	CDK9 (150-276) fragment cloned into FLAG pcDNA5-FRT-TO vector	34
M949	CyclinT1 cloned into HA pcDNA5-FRT-TO vector	34
M996	STUB1 cloned into FLAG pcDNA5-FRT-TO vector	This study
M1021	STUB1 cloned into HA pcDNA5-FRT-TO vector	This study
M1259	CDK9 K3A mutant cloned into FLAG pcDNA5-FRT-TO vector	This study
M1260	CDK9 K18, 21, 24 A mutant cloned into FLAG pcDNA5-FRT-TO vector	This study
M1261	CDK9 K3, 18, 21, 24 A mutant cloned into FLAG pcDNA5-FRT-TO vector	This study
M1262	CDK9 K35, 40, 44, 48, 49 R cloned into FLAG pcDNA5-FRT-TO vector	This study
M1263	CDK9 K44, 48, 49, 56 R cloned into FLAG pcDNA5-FRT-TO vector	This study
M1296	STUB1 H260Q mutant cloned in HA pcDNA5-FRT-TO vector	This study
M1297	STUB1 K30A mutant cloned in HA pcDNA5-FRT-TO vector	This study
M1323	STUB1 (1-225) fragment cloned into FLAG pcDNA5-FRT-TO vector	This study
M1324	STUB1 (1-127) fragment cloned into FLAG pcDNA5-FRT-TO vector	This study
M1325	STUB1 (60-303) fragment cloned into FLAG pcDNA5-FRT-TO vector	This study
M1326	STUB1 (94-303) fragment cloned into FLAG pcDNA5-FRT-TO vector	This study

TABLE 2 List of shRNA constructs used

Name of plasmid	Description	Source
S147	STUB1 shRNA #1 cloned into pLKO.1 puro vector	This study
S148	STUB1 shRNA #2 cloned into pLKO.1 puro vector	This study
S149	STUB1 shRNA #3 cloned into pLKO.1 puro vector	This study

TABLE 3 List of oligonucleotide sequences for generation of shRNA constructs

Gene	Sequence	
	Upper	Lower
STUB1 sh#1	CCGGTGCCGCCACTATCTGTGTAATCTCGAGATTACACAGA TAGTGGCGGCATTTTTG	AATTCAAAAATGCCGCCACTATCTGTGTAATCTCGAGATTA CACAGATAGTGGCGGCA
STUB1 sh#2	CCGGGGAGATGGAGAGCTATGATGACTCGAGTCATCATAGCTCT CCATCTCCTTTTTG	AATTCAAAAAGGAGATGGAGAGCTATGATGACTCGAGTCATCAT AGCTCTCCATCTCC
STUB1 sh#3	CCGGGGCTATGAAGGAGGTTATTGACTCGAGTCAATAACCTCCTT CATAGCCTTTTTG	AATTCAAAAAGGCTATGAAGGAGGTTATTGACTCGAGTCAATAAC CTCCTTCATAGCC

TABLE 4 List of primers for RNA analysis

Gene Name	Forward primer sequence	Reverse primer sequence
ADAP2	GTCTGCAGTACCTAAAAATG	AGTGGGTTCTTGTAATAGAG
APOE	GCGGATGGAGGAGATG	CTCGAACCAGCTCTTG
ATF2	GTACCAGGCCCATTTCCTCTTC	GAACGAGTGGGACTGCAGCTG
β-Actin	AGAGCTACGAGCTGCCTGAC	AGCACTGTGTTGGCGTACAG
CCND1	TCTAAGATGAAGGAGACCAT	GGAAGTGTTCAATGAAATCG
CCNE2	GCTGGCCTATGTGACTTACC	GGTAGACTTCGATGGGCCC
CDC25b	GGCACATCAAGACTGCGG	GGTAGTCGTTGACAGCACG
CDKN1A	GGACAGCAGAGGAAGACCATG	CTGTCATGCTGGTCTGCC
CDKN1B	CGACGATTCTTCTACTCAA	TTACGTTTGACGTCTTCTG
CDK6	GGAGTGTTGGCTGCATATTTG	CGATATCTGTTACAAACTTC
CDK9	GCATCATGGCAGAGATGTG	GTTGTCCACGTTTGGCC
CRABP2	GAGGGAGACACTTTCTAC	GCTCACAGACCATTTTATTC
CREB5	GAAGGCTGCATTGACTCACCAC	GTGCATGTGATGGTGTGGCGTC
E2F2	GGAGCCGGACAGTCCTTC	GCTGTCAGTAGCCTCCAAG
GAPDH	CATCACCATCTTCCAGGAG	GTTCACACCCATGACGAAC
MAP2	AATAGACCTAAGCCATGTGACATCC	AGAACCAACTTTAGCTTGGGCC
MYC	GCTTGTACCTGCAGGATC	GACTCCGTCGAGGAGAG
SFMBT1	GAGATAGTGAAAACAGCAG	CTTTCCGTAATAGTGTGTG
TAF4	GACGACAGATATGAGCAGG	GTTGCTGCATCTCCTTTG
TM2D2	GGACACTACTTCATAACCAC	AATAAGGTCAACAAACCACC
TSPAN5	CATATTTGGCTTCAATGTC	ATCCCAAAATGAACATCAC
18s rRNA	GTAACCCGTTGAACCCCATT	CCATCCAATCGGTAGTAGCG

TABLE 5 List of primers used in ChIP analyses

Gene Name	Forward primer sequence	Reverse primer sequence
CCND1 (promoter proximal)	CGGGCTTTGATCTTTGCTTA	CTGCTGCTCGCTGCTACT
C-MYC (promoter proximal)	TCCTCTCTCGCTAATCTCCGC	GGGTCCTCAGCCGTCCAGAC
CDK6 (promoter proximal)	GGAGAGAGTGCTGGTAACTCC	CGCACAGCTCCTCACCTGAG
TSPAN5 (promoter proximal)	CCTCCTTCCTGCTGGGTTC	AGCGAGAGGCGGGCGGAGCGA
C-MYC (~3 kb downstream of TSS)	GACTCTGGTAAGCGAAGC	TCCAGATCTGCTATCTCTCC
CCND1 (~3 kb downstream of TSS)	CTCCTTAGGTGACCCTGG	GACAAACAATCCAGGGCCT
CDK6 (~3 kb downstream of TSS)	GAGGTCTCTCCATCCAGCTTCTG	GGTGCGCTCAACTAGCTGG

TABLE 6 List of antibodies used

Antibody	Source(s)
STUB1	Cell Signaling Technology
Rpb1	Cell Signaling Technology
Phospho-Rpb1 CTD (Serine 2)	Cell Signaling Technology
Phospho-Rpb1 CTD (Serine 5)	Cell Signaling Technology
Ubiquitin	Cell Signaling Technology
HDAC1	Cell Signaling Technology
ELL	Cell Signaling Technology
CDK9	Santa Cruz Biotechnology
CyclinT1	Santa Cruz Biotechnology
EAF1	Santa Cruz Biotechnology
FLAG epitope tag	Sigma
HA epitope tag	Santa Cruz Biotechnology
GFP epitope tag	Biobharati Life Science
AF9	Bethyl Laboratories
Hsp70	Biobharati Life Science
β-Actin	Biobharati Life Science
HRP-conjugated secondary antibody (rabbit)	Cell Signaling Technology
HRP-conjugated secondary antibody (mouse)	Bio-Rad

concentration) to increase the efficiency of viral transduction. 24 h after transduction, old media was discarded and fresh media containing puromycin (Gibco, USA) was added (3 μg/mL final concentration) for selection of transduced cells. One more round of media change was given to the selected cells on the subsequent day. Knockdown efficiency was checked through RNA analysis by qRT-PCR as well as protein analysis by Western blotting.

Generation of expression plasmids. STUB1 cDNA sequence was cloned into suitable epitope tag-containing pcDNA/FRT/TO plasmids (Thermo Fisher Scientific, USA). Plasmids containing cDNA sequences of CDK9, ELL, AF9, AFF1, CyclinT1 and BRD4 were purchased from Open Biosystems, USA and were cloned subsequently into appropriate expression vectors as per the requirement. QuikChange II site-directed mutagenesis kit (Agilent Technologies, USA) was used for introducing mutations in plasmids.

Purification of recombinant proteins. HEK-293T cells were transfected with plasmids expressing target proteins of interest. 48 h after transfection, cells were harvested and lysed in BC1000 buffer (20 mM Tris-Cl, pH 8.0; 1000 mM KCl; 2 mM EDTA; 20% glycerol; 0.1% NP-40). Target proteins were immunoprecipitated (described below) using either anti-FLAG M2 agarose beads (Sigma, USA) or anti-HA agarose beads (Sigma, USA). FLAG-tagged proteins were eluted by incubating them with 3X-FLAG peptide (150 ng/μL final concentration) for 1 h. Bead-bound HA-tagged protein was directly used for interaction analyses along with FLAG-peptide-eluted protein. Purification was checked by SDS-PAGE followed by Coomassie staining.

Immunoprecipitation analysis. In case of epitope-tagged proteins, cells were transfected with plasmids expressing the desired proteins and harvested 48 h post-transfection. Harvested cells were lysed for 2 h at 4°C in BC150 buffer (20 mM Tris-Cl, pH 8.0, 150 mM KCL, 2 mM EDTA, 20% glycerol, 0.1% NP-40), unless mentioned otherwise. Lysed samples were centrifuged for 15 min at 12,000 rpm at 4°C and clear supernatant that contains proteins, was transferred into new vials. Proteins were immunoprecipitated by incubating lysates with either anti-FLAG M2 agarose beads (Sigma, USA) or anti-HA agarose beads (Sigma, USA) for 12 h at 4°C in a rotor with a constant rotation at 16 rpm. Next day, beads were washed three times (5 min each) using BC150 buffer and subsequently the bead-bound proteins were eluted in 1X SDS loading dye by incubating at 95°C for 10 min.

For immunoprecipitation of endogenous proteins, target-specific antibodies were used for pulling down specific proteins and IgG antibody was used as a negative control. Proteins lysates were prepared from HEK-293T cells as mentioned earlier. Lysates were pre-cleared using Protein-G magnetic beads (Sigma, USA) for 2 h at 4°C before being used for immunoprecipitation. In parallel, in separate vials, Protein-G magnetic beads were blocked using BC150 buffer containing 1% BSA for 2 h at 4°C. Pre-blocked beads were washed twice (5 min each) using BC150 buffer at 4°C. Washed beads were incubated with factor-specific antibodies and pre-cleared protein lysates for 12 h at 4°C in a rotor with a constant rotation at 16 rpm. Next day, protein-bound beads were washed three times (5 min each) using BC150 buffer and eluted in 1X SDS loading dye by incubating at 95°C for 10 min.

***In vitro* interaction analysis.** Bait proteins were immobilized on epitope tag-specific agarose beads and prey proteins were added in a reaction buffer along with bead-bound bait proteins, incubating for 12 h at 4°C in a rotor with a constant rotation at 16 rpm in BC150 buffer. Next day, protein-bound beads were washed three times (5 min each) using BC150 buffer and eluted in 1X SDS loading dye by incubating at 95°C for 10 min. Eluted proteins were subjected to Western blot analysis for checking interactions between bait and prey proteins.

Cycloheximide (CHX) chase assay. Thirty-six hours after transfection with plasmids expressing target proteins, CHX (Sigma, USA) was added to cells with a final concentration as mentioned in the figures. Cells were collected at specific time points and were lysed using BC150 buffer as mentioned before. Proteins lysates were analyzed by Western blot analysis for identifying indicated target proteins as mentioned in the figures.

Western blotting. Proteins were resolved by SDS-PAGE at 100 V for required time and were subsequently transferred to nitrocellulose membrane (Bio-Rad, USA) at 100 V for 2–3 h. Protein-bound membrane was blocked for 1 h at room temperature by using 5% skimmed milk suspension in phosphate buffer saline with 0.1% Tween 20 (PBST). Blocked membrane was incubated with factor-specific primary antibody (1:2000 dilution in PBST) for 12 h at 4°C. Next day, antibody-bound membrane was washed three times (10 min each time) with 1X PBST at room temperature. The washed membrane was subsequently incubated with HRP-conjugated anti-rabbit or anti-mouse secondary antibody (1:5000 dilution in 5% milk suspension in PBST) for 1 h at room temperature. Subsequently, membrane was washed three times (10 min each time) using 1X PBST at room temperature. Protein bands were visualized using Clarity Western ECL substrate (Bio-Rad, USA) on the iBright imaging system (Thermo Fisher, USA).

RNA extraction and qRT-PCR analysis. Total RNA was isolated from cells using TRIzol (Invitrogen, USA) as per manufacturer's protocol. Subsequently, cDNA synthesis was performed using isolated RNA using Verso cDNA synthesis kit (Thermo Scientific, USA) following the manufacturer's protocol. The synthesized cDNA was diluted 100 times before being subjected to qRT-PCR analysis. qRT-PCR was done using iTaq universal SYBR green supermix (Bio-Rad, USA) and target-specific primers on the CFX96 real-time PCR detection system (Bio-Rad, USA).

Chromatin immunoprecipitation (ChIP) analysis. ChIP analysis was carried out following the earlier described protocol.[3,42] Cells were crosslinked using 1% formaldehyde for 10 min at room temperature. Crosslinking was stopped by using 125 mM glycine solution in 1X PBS for 10 min at room temperature. Crosslinked cells were lysed in lysis buffer (0.5% NP40, 1% Triton X-100, 300 mM NaCl, 20 mM Tris pH 7.5, 2 mM EDTA) for 30 min on ice. Lysed cells were passed through 23-gauge syringe for 10 times (for each sample). After that, passaged cells were centrifuged for 10 min at 5000 rpm at 4°C. Subsequently, the precipitated nuclear pellet was resuspended in ChIP shearing buffer (1% SDS, 10 mM EDTA and 500 mM Tris pH 8.0)

and chromatin was sheared using Bioruptor^{TM} UCD200 (Diagenode) sonicator for 20 min (30 s on or off pulses in between). Sheared lysate was centrifuged for 10 min at 12000 rpm at 4°C and the supernatant was transferred into a fresh vial. The supernatant was diluted 10 times using dilution buffer (0.01% SDS, 1.1% Triton X-100, 1.1 mM EDTA, 20 mM Tris-Cl pH 8.0, 167 mM NaCl). An appropriate amount of diluted sample was pre-cleared using Protein-G magnetic beads (Sigma, USA) for 2 h at 4°C. Pre-cleared lysate was incubated with 2 μg of factor-specific antibody for 12 h at 4°C. In a parallel analysis, Protein-G magnetic beads were blocked using salmon sperm DNA (Invitrogen, USA) in ChIP dilution buffer for 12 h at 4°C. Next day, blocked beads were incubated with antibody-bound protein lysate for 4 h at 4°C. Protein antibody complex-bound beads were subjected to four washing steps. Each washing was done for 5 min at 4°C. First washing was performed with low salt buffer (0.1% SDS, 1% Triton X-100, 2 mM EDTA, 20 mM Tris-Cl pH 8.0, 150 mM NaCl). Second washing was performed with high salt buffer (0.1% SDS, 1% Triton X-100, 2 mM EDTA, 20 mM Tris-Cl pH 8.0, 500 mM NaCl). Third washing was performed with lithium chloride buffer (0.5% LiCl, 1% NP-40, 1% deoxycholate, 20 mM Tris-Cl pH 8.0 and 1 mM EDTA). Finally, fourth washing was performed with TE buffer. Subsequently complex bound DNA was eluted from beads by adding elution buffer (1% SDS, 0.1 M $NaHCO_3$) and vortexing the beads every after 5 min (10 s each time) for 2 h. Eluted supernatant was transferred to a fresh vial and DNA was separated from the complex by increasing the NaCl concentration to 200 mM and incubating the solution at 65°C for 12 h. After that, proteins in the solution were digested using Proteinase K for 1 h at 45°C. DNA was purified using PCR purification Kit (Qiagen, Germany) following manufacturer's protocol. The eluted DNA was analyzed using iTaq universal SYBR green supermix (Bio-Rad, USA) and target gene-specific primers on the CFX96 real-time PCR detection system (Bio-Rad, USA).

Mass spectrometry analysis. The mass spectrometry analysis for identifying CDK9-associated proteins have been performed as mentioned in our earlier study.[3]

Quantification and statistical analysis. All the RNA expression and ChIP data presented in this study, represent mean ± SD from minimum of two biological and three technical replicates. Statistical analysis was done using GraphPad Prism (version 5.0) software. *P*-value was calculated using one-tailed Student's *t* test where ns denotes not significant, * denotes $P \leq 0.05$, ** denotes $P \leq 0.01$, *** denotes $P \leq 0.001$.

ACKNOWLEDGEMENTS

The work as described in this study was supported by a CSIR focused basic research (FBR) project, MLP141 and DST extramural funding (EMR/2016/001593) awarded to DB as well as CSIR-IICB internal funding through P07 budget head. SB is a recipient of UGC Senior Research Fellowship. AN and AG are the recipients of CSIR Senior Research Fellowship. DPM is a recipient of Dept. of Biotechnology Senior Research Fellowship.

AUTHOR CONTRIBUTIONS

SB, AN, and AG performed majority of the experiments in consultation with DB. DPM made important contribution in the P-TEFb overexpression analysis and its effect on target gene expression. AN, AG, and DB consulted and wrote the manuscript. SB, AN, and AG also helped in editing the manuscript.

FUNDING

Council of Scientific and Industrial Research(CSIR) - Indian Institute of Chemical Biology(IICB) internal funding through P07, India.

ORCID

Debabrata Biswas http://orcid.org/0000-0002-6782-6398

DATA AVAILABILITY STATEMENT

The entire set of original raw images of Western blots that were used for making figures as described in this study is available through Mendeley data repository through https://data.mendeley.com/datasets/zg89v9sfkz/1.

REFERENCES

1. Basu S, Nandy A, Biswas D. Keeping RNA polymerase II on the run: Functions of MLL fusion partners in transcriptional regulation. Biochim Biophys Acta Gene Regul Mech. 2020;1863:194563. doi:10.1016/j.bbagrm.2020.194563. PMID: 32348849.
2. Bres V, Yoh SM, Jones KA. The multi-tasking P-TEFb complex. Curr Opin Cell Biol. 2008;20:334–340. doi:10.1016/j.ceb.2008.04.008.
3. Ghosh K, Tang M, Kumari N, Nandy A, Basu S, Mall DP, Rai K, Biswas D. Positive regulation of transcription by human ZMYND8 through Its association with P-TEFb complex. Cell Rep. 2018;24:2141–2154 e6. doi:10.1016/j.celrep.2018.07.064. PMID: 30134174.
4. Peng J, Zhu Y, Milton JT, Price DH. Identification of multiple cyclin subunits of human P-TEFb. Genes Dev. 1998;12:755–762. doi:10.1101/gad.12.5.755. PMID: 9499409.
5. Price DH. P-TEFb, a cyclin-dependent kinase controlling elongation by RNA polymerase II. Mol Cell Biol. 2000;20:2629–2634. doi:10.1128/MCB.20.8.2629-2634.2000. PMID: 10733565.

6. Yang Z, Zhu Q, Luo K, Zhou Q. The 7SK small nuclear RNA inhibits the CDK9/cyclin T1 kinase to control transcription. Nature. 2001;414:317–322. doi:10.1038/35104575. PMID: 11713532.
7. Yik JH, Chen R, Nishimura R, Jennings JL, Link AJ, Zhou Q. Inhibition of P-TEFb (CDK9/Cyclin T) kinase and RNA polymerase II transcription by the coordinated actions of HEXIM1 and 7SK snRNA. Mol Cell. 2003;12:971–982.
8. Sessler RJ, Noy N. A ligand-activated nuclear localization signal in cellular retinoic acid binding protein-II. Mol Cell. 2005;18:343–353. doi:10.1016/j.molcel.2005.03.026. PMID: 15866176.
9. Yang Z, Yik JH, Chen R, He N, Jang MK, Ozato K, Zhou Q. Recruitment of P-TEFb for stimulation of transcriptional elongation by the bromodomain protein Brd4. Mol Cell. 2005;19:535–545. doi:10.1016/j.molcel.2005.06.029. PMID: 16109377.
10. Biswas D, Milne TA, Basrur V, Kim J, Elenitoba-Johnson KS, Allis CD, Roeder RG. Function of leukemogenic mixed lineage leukemia 1 (MLL) fusion proteins through distinct partner protein complexes. Proc Natl Acad Sci U S A. 2011;108:15751–15756. doi:10.1073/pnas.1111498108. PMID: 21896721.
11. He N, Chan CK, Sobhian B, Chou S, Xue Y, Liu M, Alber T, Benkirane M, Zhou Q. Human polymerase-associated factor complex (PAFc) connects the super elongation complex (SEC) to RNA polymerase II on chromatin. Proc Natl Acad Sci U S A. 2011;108:E636–E645. doi:10.1073/pnas.1107107108. PMID: 21873227.
12. Mayer A, Landry HM, Churchman LS. Pause & go: from the discovery of RNA polymerase pausing to its functional implications. Curr Opin Cell Biol. 2017;46:72–80. doi:10.1016/j.ceb.2017.03.002. PMID: 28363125.
13. Kiernan RE, Emiliani S, Nakayama K, Castro A, Labbe JC, Lorca T, Nakayama Ki K, Benkirane M. Interaction between cyclin T1 and SCF(SKP2) targets CDK9 for ubiquitination and degradation by the proteasome. Mol Cell Biol. 2001;21:7956–7970. doi:10.1128/MCB.21.23.7956-7970.2001. PMID: 11689688.
14. Barboric M, Zhang F, Besenicar M, Plemenitas A, Peterlin BM. Ubiquitylation of Cdk9 by Skp2 facilitates optimal Tat transactivation. J Virol. 2005;79:11135–11141. doi:10.1128/JVI.79.17.11135-11141.2005. PMID: 16103164.
15. Zhang S, Hu ZW, Mao CY, Shi CH, Xu YM. CHIP as a therapeutic target for neurological diseases. Cell Death Dis. 2020;11:727. doi:10.1038/s41419-020-02953-5. PMID: 32908122.
16. Li L, Xin H, Xu X, Huang M, Zhang X, Chen Y, Zhang S, Fu XY, Chang Z. CHIP mediates degradation of Smad proteins and potentially regulates Smad-induced transcription. Mol Cell Biol. 2004;24:856–864. doi:10.1128/MCB.24.2.856-864.2004. PMID: 14701756.
17. Xu W, Marcu M, Yuan X, Mimnaugh E, Patterson C, Neckers L. Chaperone-dependent E3 ubiquitin ligase CHIP mediates a degradative pathway for c-ErbB2/Neu. Proc Natl Acad Sci U S A. 2002;99:12847–12852. doi:10.1073/pnas.202365899. PMID: 12239347.
18. Shimura H, Schwartz D, Gygi SP, Kosik KS. CHIP-Hsc70 complex ubiquitinates phosphorylated tau and enhances cell survival. J Biol Chem. 2004;279:4869–4876. doi:10.1074/jbc.M305838200. PMID: 14612456.
19. Urushitani M, Kurisu J, Tateno M, Hatakeyama S, Nakayama K, Kato S, Takahashi R. CHIP promotes proteasomal degradation of familial ALS-linked mutant SOD1 by ubiquitinating Hsp/Hsc70. J Neurochem. 2004;90:231–244. doi:10.1111/j.1471-4159.2004.02486.x. PMID: 15198682.
20. Huang Z, Nie L, Xu M, Sun XH. Notch-induced E2A degradation requires CHIP and Hsc70 as novel facilitators of ubiquitination. Mol Cell Biol. 2004;24:8951–8962. doi:10.1128/MCB.24.20.8951-8962.2004. PMID: 15456869.
21. Peng HM, Morishima Y, Jenkins GJ, Dunbar AY, Lau M, Patterson C, Pratt WB, Osawa Y. Ubiquitylation of neuronal nitric-oxide synthase by CHIP, a chaperone-dependent E3 ligase. J Biol Chem. 2004;279:52970–52977. doi:10.1074/jbc.M406926200. PMID: 15466472.
22. Shin Y, Klucken J, Patterson C, Hyman BT, McLean PJ. The co-chaperone carboxyl terminus of Hsp70-interacting protein (CHIP) mediates alpha-synuclein degradation decisions between proteasomal and lysosomal pathways. J Biol Chem. 2005;280:23727–23734. doi:10.1074/jbc.M503326200. PMID: 15845543.
23. Hwang JR, Zhang C, Patterson C. C-terminus of heat shock protein 70-interacting protein facilitates degradation of apoptosis signal-regulating kinase 1 and inhibits apoptosis signal-regulating kinase 1-dependent apoptosis. Cell Stress Chaperones. 2005;10:147–156. doi:10.1379/csc-90r.1. PMID: 16038411.
24. Kim SA, Yoon JH, Kim DK, Kim SG, Ahn SG. CHIP interacts with heat shock factor 1 during heat stress. FEBS Lett. 2005;579:6559–6563. doi:10.1016/j.febslet.2005.10.043. PMID: 16293251.
25. Dai Q, Zhang C, Wu Y, McDonough H, Whaley RA, Godfrey V, Li HH, Madamanchi N, Xu W, Neckers L, et al. CHIP activates HSF1 and confers protection against apoptosis and cellular stress. embo J. 2003;22:5446–5458. doi:10.1093/emboj/cdg529. PMID: 14532117.
26. Qian SB, McDonough H, Boellmann F, Cyr DM, Patterson C. CHIP-mediated stress recovery by sequential ubiquitination of substrates and Hsp70. Nature. 2006;440:551–555. doi:10.1038/nature04600. PMID: 16554822.
27. Zhan S, Wang T, Ge W. Multiple functions of the E3 ubiquitin ligase CHIP in immunity. Int Rev Immunol. 2017;36:300–312. doi:10.1080/08830185.2017.1309528. PMID: 28574736.
28. Zhou P, Fernandes N, Dodge IL, Reddi AL, Rao N, Safran H, DiPetrillo TA, Wazer DE, Band V, Band H. ErbB2 degradation mediated by the co-chaperone protein CHIP. J Biol Chem. 2003;278:13829–13837. doi:10.1074/jbc.M209640200. PMID: 12574167.
29. Kajiro M, Hirota R, Nakajima Y, Kawanowa K, So-Ma K, Ito I, Yamaguchi Y, Ohie SH, Kobayashi Y, Seino Y, et al. The ubiquitin ligase CHIP acts as an upstream regulator of oncogenic pathways. Nat Cell Biol. 2009;11:312–319. doi:10.1038/ncb1839. PMID: 19198599.
30. Wang S, Wu X, Zhang J, Chen Y, Xu J, Xia X, He S, Qiang F, Li A, Shu Y, et al. CHIP functions as a novel suppressor of tumour angiogenesis with prognostic significance in human gastric cancer. Gut. 2013;62:496–508. doi:10.1136/gutjnl-2011-301522. PMID: 22535373.
31. Tang DE, Dai Y, Lin LW, Xu Y, Liu DZ, Hong XP, Jiang HW, Xu SH. STUB1 suppresseses tumorigenesis and chemoresistance through antagonizing YAP1 signaling. Cancer Sci. 2019;110:3145–3156. doi:10.1111/cas.14166. PMID: 31393050.
32. Xu S, Fan L, Jeon HY, Zhang F, Cui X, Mickle MB, Peng G, Hussain A, Fazli L, Gleave ME, et al. p300-mediated acetylation of histone demethylase JMJD1A prevents its degradation by ubiquitin ligase STUB1 and enhances its activity in prostate cancer. Cancer Res. 2020;80:3074–3087. doi:10.1158/0008-5472.CAN-20-0233. PMID: 32522824.
33 Sarkar S, Brautigan DL, Parsons SJ, Larner JM. Androgen receptor degradation by the E3 ligase CHIP modulates mitotic arrest in prostate cancer cells. Oncogene. 2014;33:26–33. doi:10.1038/onc.2012.561. PMID: 23246967.
34. Mall DP, Basu S, Ghosh K, Kumari N, Lahiri A, Paul S, Biswas D. Human FKBP5 negatively regulates transcription through inhibition of P-TEFb complex formation. Mol Cell Biol. 2022;42:e0034421. doi:10.1128/MCB.00344-21. PMID: 34780285.
35. Basu S, Barad M, Yadav D, Nandy A, Mukherjee B, Sarkar J, Chakrabarti P, Mukhopadhyay S, Biswas D. DBC1, p300, HDAC3, and Siah1 coordinately regulate ELL stability and function for expression of its target genes. Proc Natl Acad Sci U S A. 2020;117:6509–6520. doi:10.1073/pnas.1912375117. PMID: 32152128.
36. He N, Liu M, Hsu J, Xue Y, Chou S, Burlingame A, Krogan NJ, Alber T, Zhou Q. HIV-1 Tat and host AFF4 recruit two transcription elongation factors into a bifunctional complex for coordinated activation of HIV-1 transcription. Mol Cell. 2010;38:428–438. doi:10.1016/j.molcel.2010.04.013. PMID: 20471948.
37. Udeshi ND, Mani DR, Eisenhaure T, Mertins P, Jaffe JD, Clauser KR, Hacohen N, Carr SA. Methods for quantification of in vivo changes in protein ubiquitination following proteasome and deubiquitinase inhibition. Mol Cell Proteomics. 2012;11:148–159. doi:10.1074/mcp.M111.016857. PMID: 22505724.
38. Udeshi ND, Mertins P, Svinkina T, Carr SA. Large-scale identification of ubiquitination sites by mass spectrometry. Nat Protoc. 2013;8:1950–1960. doi:10.1038/nprot.2013.120. PMID: 24051958.
39. Udeshi ND, Svinkina T, Mertins P, Kuhn E, Mani DR, Qiao JW, Carr SA. Refined preparation and use of anti-diglycine remnant (K-epsilon-GG) antibody enables routine quantification of 10,000s of ubiquitination sites in single proteomics experiments. Mol Cell Proteomics. 2013;12:825–831. doi:10.1074/mcp.O112.027094. PMID: 23266961.
40. Somesh BP, Reid J, Liu WF, Sogaard TM, Erdjument-Bromage H, Tempst P, Svejstrup JQ. Multiple mechanisms confining RNA polymerase II ubiquitylation to polymerases undergoing transcriptional arrest. Cell. 2005;121:913–923. doi:10.1016/j.cell.2005.04.010. PMID: 15960978.
41. Yadav D, Ghosh K, Basu S, Roeder RG, Biswas D. Multivalent role of human TFIID in recruiting elongation components at the promoter-proximal region for transcriptional control. Cell Rep. 2019;26:1303–1317 e7. doi:10.1016/j.celrep.2019.01.012. PMID: 30699356.
42. Kumari N, Hassan MA, Lu X, Roeder RG, Biswas D. AFF1 acetylation by p300 temporally inhibits transcription during genotoxic stress response. Proc Natl Acad Sci USA. 2019;116:22140–22151. doi:10.1073/pnas.1907097116. PMID: 31611376.
43 Basu S, Nandy A, Barad MK, Pal S, Biswas D. Negative feedback loop mechanism between EAF1/2 and DBC1 in regulating ELL stability and

functions. Mol Cell Biol. 2022;42:e0015122. doi:10.1128/mcb.00151-22. PMID: 36036574.
44. Elia AE, Boardman AP, Wang DC, Huttlin EL, Everley RA, Dephoure N, Zhou C, Koren I, Gygi SP, Elledge SJ. Quantitative proteomic atlas of ubiquitination and acetylation in the DNA damage response. Mol Cell. 2015;59:867–881. doi:10.1016/j.molcel.2015.05.006. PMID: 26051181.
45. Svinkina T, Gu H, Silva JC, Mertins P, Qiao J, Fereshetian S, Jaffe JD, Kuhn E, Udeshi ND, Carr SA. Deep, quantitative coverage of the lysine acetylome using novel anti-acetyl-lysine antibodies and an optimized proteomic workflow. Mol Cell Proteomics. 2015;14:2429–2440. doi:10.1074/mcp.O114.047555. PMID: 25953088.
46. Li D, Marchenko ND, Schulz R, Fischer V, Velasco-Hernandez T, Talos F, Moll UM. Functional inactivation of endogenous MDM2 and CHIP by HSP90 causes aberrant stabilization of mutant p53 in human cancer cells. Mol Cancer Res. 2011;9:577–588. doi:10.1158/1541-7786.MCR-10-0534. PMID: 21478269.